UNIVERSIDADE FEDERAL DE MINAS GERAIS

Programa de Pós-Graduação em Engenharia Metalúrgica, Materiais e de Minas

Dissertação de Mestrado

EFEITO DE TRATAMENTOS TÉRMICOS NO COMPORTAMENTO EM FADIGA DE FIOS DE NiTi SUPERELÁSTICOS

Autora: Jéssica Dornelas Silva

Orientador: Prof. Dr. Vicente Tadeu Lopes Buono

Fevereiro / 2019

Jéssica Dornelas Silva

Efeito de Tratamentos Térmicos no Comportamento em Fadiga de Fios de NiTi Superelásticos

Dissertação apresentada ao Programa de Pós-Graduação em Engenharia Metalúrgica, Materiais e de Minas da Escola de Engenharia da Universidade Federal de Minas Gerais, como requisito parcial para obtenção do Grau de Mestre em Engenharia Metalúrgica, Materiais e de Minas.

Área de Concentração: Metalurgia Física.

Orientador: Prof. Vicente Tadeu Lopes Buono.

Belo Horizonte

Universidade Federal de Minas Gerais

Escola de Engenharia

2019

Silva, Jéssica Dornelas.
S586e Efeito de tratamentos térmicos no comportamento em fadiga de fios de NiTi superelásticos [manuscrito] / Jéssica Dornelas Silva. - 2019.
xi, 82 f., enc.: il.

Orientador: Vicente Tadeu Lopes Buono.

Dissertação (mestrado) - Universidade Federal de Minas Gerais, Escola de Engenharia.

Inclui bibliografia.

1. Engenharia metalúrgica -Teses. 2. Metalurgia física - Teses. 3. Efeito da memória de forma - Teses. 4. Fadiga - Teses. 5. Metais - Tratamento térmico - Teses. 6. Ligas de níquel-titânio - Teses. I. Buono, Vicente Tadeu Lopes. II. Universidade Federal de Minas Gerais. Escola de Engenharia. III. Título.

CDU: 669(043)

DEDICATÓRIA

Ao meu irmão, Pedro Henrique.

À minha princesa, Bianca.

Ao meu príncipe, Guilherme Antônio.

AGRADECIMENTOS

Agradeço ao meu orientador, professor Vicente Buono, por ser me ensinar a confiar em mim e, ao mesmo tempo, ser minha luz nas horas de desespero. Aos professores Leandro Arruda e Dagoberto Brandão por todo suporte nestes dois anos. Ao professor Geraldo, pelas valiosas contribuições. Ao LabTerm e agregados, pela parceria, convivência e paciência, em especial à Nat, à Tairine, ao Pedro, à Su e à Paula.

Aos meus pais, Neide e João Pedro, minha base de tudo. Ao meu irmão, minha maior inspiração. Ao Matheus, por estar sempre do meu lado incondicionalmente. À minha família e à família Camelo-Cruz.

Àqueles que eu não abro mão e que me acompanharam por mais uma jornada: Júlia, Luiza e Ricardo; Glenda, Camila e Fafi; Túlio, Felipe e Ítalo; Lari, Jacque, Glau e Deh; Sílvia, Gaby, Bárbara, Jô, Luisa, Túlio D. , Mari e Zé V.; e, por fim, mas não menos importante, Ana, Isa, Amanda, Madruga e Bia.

À CAPES, ao CNPq e à FAPEMIG pelo apoio financeiro. À UFMG e à Escola de Engenharia por toda estrutura e excelência.

SUMÁRIO

LISTA DE FIGURAS

LISTA DE TABELAS

LISTA DE NOTAÇÕES

Af - Temperatura de final de transformação martensítica reversa.

As - Temperatura de início de transformação martensítica reversa.

DRX - Difração de raios x.

DSC - Calorimetria diferencial exploratória.

EMF - Efeito memória de forma.

LMF - Liga com memória de forma.

MEV - Microscópio eletrônico de varredura.

Mf - Temperatura de fim de transformação martensítica.

MIT - Martensita induzida por tensão.

Ms - Temperatura de início de transformação martensítica.

MT - Martensitic transformation.

RT - Reverse martensitic transformation.

SE - Superelasticidade.

SE - Superelasticity.

SME - Shape memory effect.

TM - Transformação martensítica.

TR - Transformação reversa.

RESUMO

Ligas aproximadamente equiatômicas NiTi com pequeno excesso de Ni são ligas funcionais de grande relevância comercial. Durante seu uso, estas ligas podem estar frequentemente sujeitas a esforços cíclicos e, consequentemente, à fratura por fadiga. Este trabalho tem como motivação principal o uso de NiTi em limas endodônticas, as quais estão sujeitas a condições agressivas de deformação cíclicas. Atualmente, esforços tem sido feitos na otimização do design destas limas e na realização de tratamentos térmicos nos fios a partir das quais elas são fabricadas ou nas próprias limas após sua usinagem, produzindo limas de propriedades ainda superiores às das tradicionais superelásticas. Entretanto, maiores entendimentos sobre os tratamentos realizados e sobre os mecanismos de fadiga ainda são escassos. Neste contexto, este trabalho tem como objetivo contribuir para a compreensão metalúrgica dos efeitos mecânicos obtidos por meio de tratamentos térmicos em fios de superelásticos de NiTi, relacionando a microestrutura obtida por meio destes tratamentos e as propriedades mecânicas resultantes em condições agressivas de fadiga. Para isto, tratamentos térmicos foram realizados em diferentes temperaturas e a resistência em fadiga de baixo ciclo foi avaliada. Ensaios de tração e difratometria de raios X foram realizados para caracterização mecânica e microestrutural, respectivamente, e análise calorimétrica diferencial exploratória, para determinação das temperaturas de transformação. Os ensaios de fadiga foram realizados em equipamento de flexão rotativa adequado em temperatura controlada. Posteriormente, as condições de tratamento térmico que resultaram nas maiores vidas em fadiga foram repetidas e ensaios de fadiga em diferentes amplitudes de deformação e em temperaturas distintas foram realizados para avaliar a influência destas variáveis bem como o efeito das fases presentes dado um estado termomecânico fixo. Os resultados obtidos mostram que tratamentos térmicos são efetivos para melhoria da resistência à fadiga especialmente quando se tem a presença da fase R. Esta melhoria foi atribuída ao comportamento de diferentes microestruturas durante a ciclagem mecânica e a diferenças na propagação da trinca: enquanto fios austeníticos passam por um grande acúmulo de defeitos, fios constituídos por fase R têm trincas ramificadas através dos contornos de variantes.

Palavras-chave: NiTi, memória de forma, tratamentos térmicos, fadiga.

ABSTRACT

Near-equiatomic NiTi alloys rich in Ni are functional alloys of great commercial relevance. Within their applications, these alloys are commonly subjected to cyclic efforts and, thus, to failure by fatigue. Este trabalho tem como motivação principal o uso de limas endodônticas, as quais estão sujeitas a condições agressivas de deformação cíclicas. The present work has as motivation the use of NiTi in endodontic files, which undergo aggressive conditions of cyclic deformation. Efforts have currently being made in the files design optimization and heat treatment performance in the wires from which they are manufactured or in the files themselves, producing instruments with an even higher performance than the traditional superelastic instruments. However, a better understating about the performed heat-treatments and the fatigue mechanisms are still scarce. In this context, this work has the aim of contributing to a better metallurgical comprehension of the mechanical effects obtained through heat-treatments of near equiatomic NiTi wires rich in Ni, relating ageing heat-treatments, the microstructure achieved through them and the resultant mechanical properties in an aggressive fatigue condition. For that, annealing heat treatments have been performed in diferent temperatures and the low cycle fatigue life was evaluated. Tension testes and X-ray diffractometry were performed for mechanical and microstructural characterization, respectively, and differential scanning calorimetry was realized to determinate the transformation temperatures. Subsequently, the heat-treatment conditions which provided the higher fatigue lives were repeated and fatigue tests in varying deformation amplitudes and temperatures were performed in order to evaluate the influence of these variables as well as the effect of the present phases for a fixed thermomechanical state. The results obtained showed that aging treatments are effective in increasing the fatigue life of superelastic NiTi wires, especially when the presence of the R-phase is achieved. These improvements were attributed to the behavior of these microstructures during mechanical cycling and to the differences during crack propagation: while austenitic wires undergo a high amount of defect accumulation, wires constituted by the R-phase have cracks ramification through the variants interfaces.

Keywords: NiTi, shape memory effect, heat-treatments, fatigue.

1. INTRODUÇÃO

O efeito memória de forma (EMF) é a capacidade que determinados materiais apresentam de recuperar sua forma original após uma deformação aparentemente permanente através de um estímulo adequado. O efeito superelástico, ou superelasticidade (SE), é um caso particular do efeito memória de forma em que a estrutura deformada recupera sua forma original simplesmente pela retirada da carga aplicada. Por meio de uma seleção de composições químicas e tratamentos térmicos adequados, uma liga com memória de forma pode apresentar um efeito ou outro em determinadas condições de trabalho (1).

Ambos os efeitos estão relacionados a uma transformação martensítica termoelástica reversível que envolve uma fase matriz austenítica de alta temperatura se transformando em uma fase martensítica de baixa temperatura. Transformações martensíticas (TM) são transformações adifusionais, cisalhantes e atérmicas, envolvendo o movimento cooperativo e simultâneo de vários átomos em distâncias menores que o parâmetro de rede durante um resfriamento contínuo. Seu início se dá no momento em que a temperatura do componente é abaixada até uma determinada temperatura crítica denominada Ms, associada à força motriz necessária para o cisalhamento da rede.

A transformação continua com o resfriamento e a estrutura se torna totalmente martensítica quando a temperatura chega à temperatura de fim de transformação martensítica Mf. Se o resfriamento for interrompido entre as temperaturas Ms e Mf, a transformação cessará e a estrutura terá um balanço entre a fase matriz e a fase martensítica formada. Dentro de um grão austenítico, a martensita formada durante o resfriamento livre de tensões, denominada martensita térmica, pode ser formada em várias orientações diferentes, sendo que cada orientação corresponde a uma variante da martensita.

No aquecimento, ocorre a transformação reversa (TR) de martensita para a fase matriz austenítica que tem início na temperatura As e fim na temperatura Af. Portanto, no ciclo de transformação está presente uma histerese térmica referente ao intervalo entre as temperaturas da transformação direta no resfriamento e da transformação reversa no aquecimento, dada pelas diferenças |Ms - Af| e |As – Mf|. Esta diferença nas temperaturas de transformação no aquecimento e no resfriamento está diretamente

relacionada às energias de natureza não-química envolvidas na TM devidas ao movimento de interfaces durante o cisalhamento da rede (2–5).

No EMF convencional, a forma original de uma estrutura pode ser recuperada após uma deformação aparentemente permanente por meio de um estímulo adequado. Neste caso, as deformações são produzidas por um mecanismo de reorientação das variantes quando uma tensão é aplicada na estrutura martensítica, induzindo uma orientação preferencial nesta fase da seguinte forma: as variantes que têm suas componentes cisalhantes alinhadas com a tensão aplicada tendem a crescer enquanto as que não estão favoravelmente orientadas tendem a se contrair, induzindo-se uma orientação preferencial na martensita, que passa a ser chamada de martensita demaclada. Quando o carregamento é interrompido e a estrutura é descarregada, a deformação produzida é mantida, ocorrendo apenas uma recuperação elástica. Ao se aquecer esta amostra acima de Af, a formação de austenita durante a TR é acompanhada da recuperação da forma original. No resfriamento, a martensita térmica será formada novamente com variantes em diversas orientações, retomando-se o estado inicial (6).

Por outro lado, na SE, a aplicação de tensões em determinados níveis críticos (σ^{Ms}) em uma estrutura inicialmente austenítica induz a formação de martensita (martensita induzida por tensão – MIT) por um cisalhamento da rede. Esta transformação martensítica induzida produz, no componente, uma deformação macroscópica. Com a retirada da tensão, a martensita se torna termicamente instável, se transforma em austenita novamente e a forma inicial é recuperada. O resultado destas transformações induzidas no carregamento e no descarregamento é que o material consegue recuperar a forma quando deformado além do limite elástico simplesmente pela retirada de tensão (7,8).

Entretanto, vale ressaltar que a transformação de martensita induzida por tensão ocorre apenas em temperaturas inferiores a uma temperatura crítica Md. Uma vez que a estabilidade de austenita é maior em maiores temperaturas, a tensão necessária para indução de martensita aumenta com o aumento de temperatura. Com isso, em temperaturas suficientemente elevadas, acima de Md, a força motriz para indução da martensita é tão alta que a austenita se deformará plasticamente antes de se atingir σ^{Ms}. Por outro lado, em temperaturas inferiores a As, a martensita induzida se manterá

estável mesmo após a retirada da tensão, não havendo recuperação de forma no descarregamento (9).

Ligas NiTi aproximadamente equiatômicas são as ligas que apresentam efeito memória de forma de maior relevância comercial. Estas ligas, que apresentam uma austenita de estrutura cristalina cúbica do tipo B2 e uma martensita de estrutura cristalina monoclínica B19', apresentam baixa anisotropia elástica, baixo módulo de elasticidade, biocompatibilidade e elevada resistência à corrosão e à abrasão se comparadas a outras ligas que apresentam efeito memória de forma. Devido às suas propriedades mecânicas associadas às propriedades funcionais de EMF e SE, elas encontram aplicações nas indústrias de atuadores, de acoplamentos, médica e odontológica (7,10–12).

Em odontologia, o uso de NiTi se tornou usual na confecção de fios ortodônticos e de limas endodônticas principalmente devido à sua grande flexibilidade e à sua baixa força de retorno, obtidas em função do baixo módulo de elasticidade, do EMF e da SE. Devido a essas propriedades, limas de NiTi são capazes de manter a forma original do canal radicular e mesmo trabalhar em movimentos rotatórios, proporcionando maior eficiência aos tratamentos endodônticos (13–15).

Entretanto, apesar das características favoráveis desta liga, os instrumentos endodônticos, ou limas, de NiTi apresentam risco de ruptura por fadiga devido ao seu movimento rotatório. A fratura por fadiga ocorre sem deformação plástica macroscópica prévia e, por isso, a lima pode se romper de forma inesperada durante o procedimento sem nenhum sinal mecânico de aviso. O rompimento da lima no interior do canal é uma complicação cirúrgica que pode comprometer o resultado do tratamento caso a extração de seus fragmentos não seja viável (16–18).

Em estudos presentes na literatura, é possível notar que a resistência à fadiga de fios NiTi é influenciada pelas fases presentes em sua microestrutura (12,16,19,20), pela presença de precipitados (21) e pelo estado de encruamento (22). Outros fatores como a temperatura de teste (23), o design do instrumento (14) e as características do canal também são relevantes (15).

Na fabricação de instrumentos endodônticos, progressos contínuos nos tratamentos térmicos realizados nos fios utilizados em sua fabricação e/ou nas limas assim como no design do instrumento levam a melhorias na flexibilidade e na resistência à fadiga com

altas amplitudes de deformação, duas propriedades essenciais durante a aplicação clínica, conforme notado por diversos autores (12,24–26). Enquanto o design tem influência na tensão máxima atingida no instrumento (27), os tratamentos térmicos determinam a microestrutura e o estado microestrutural na temperatura de utilização (25,28–30).

Sabe-se que tratamentos térmicos de envelhecimento e tratamentos termomecânicos são utilizados com sucesso no controle das temperaturas de transformação martensítica e reversa em ligas NiTi aproximadamente equiatômicas ricas em Ni. Esses tratamentos favorecem a formação de três tipos de precipitados, a depender do tempo e da temperatura de tratamento térmico na seguinte sequência de precipitação: Ti_3Ni_4, Ti_2Ni_3 e $TiNi_3$. A formação destes precipitados é acompanhada por uma diminuição do teor de Ni na matriz austenítica, relacionado com a fração de precipitados formados em uma dada temperatura. Porém, a temperatura de transformação é altamente sensível à composição química e a redução do teor de níquel na austenita leva a um aumento da temperatura de início de transformação martensítica, Ms, facilitando-a no resfriamento. Desta forma, a temperatura de tratamento determina as composições químicas de equilíbrio na matriz e no precitado e, consequentemente, a temperatura de transformação martensítica(7).

Por outro lado, a presença de campos de tensão ao redor dos precipitados intermediários e coerentes Ti_3Ni_4 favorece a formação de uma fase pré-martensítica de estrutura trigonal denominada fase R. Nestes casos, a transformação martensítica ocorre em dois estágios e a fase R, que é a fase intermediária, pode ser obtida em temperaturas determinadas. Com isso, os precipitados coerentes têm também um papel predominante no comportamento das transformações e na evolução microestrutural destas ligas. A transformação austenita B2 $\rightarrow$ fase R tem natureza martensítica e a TM em dois estágios austenita B2 $\rightarrow$ fase R $\rightarrow$ martensita B19’ está associada a menores distorções na rede em cada estágio se comparada à transformação direta austenita B2 $\rightarrow$ martensita B19’ (22,31–33).

Assim, tratamentos térmicos influenciam diretamente nas fases presentes na temperatura de trabalho e na sua estabilidade por meio de alterações nas temperaturas e na sequência de transformação e em seu estado termomecânico, sendo determinantes no controle das propriedades mecânicas e funcionais (7). Estudos realizados em instrumentos

endodônticos indicam que a presença de fase R e martensita B19’ em instrumentos tratados é benéfica para a melhoria da vida em fadiga de baixo ciclo em relação aos tradicionais instrumentos superelásticos. Entretanto, ainda não se sabe a razão pela qual estas melhorias são obtidas e tão pouco se tem conhecimento dos mecanismos de fadiga (12,25,28–30). De fato, a relação entre as melhorias na flexibilidade e na fadiga em altas deformações e as microestruturas obtidas nos tratamentos realizados não é conhecida em detalhes por estarem envolvidos simultaneamente diversos fatores e pelo papel significante do histórico de deformação plástica prévia (29,34).

Neste contexto, este trabalho tem como objetivo contribuir para um melhor entendimento do comportamento metalúrgico e mecânico de fios NiTi aproximadamente equiatômicos com pequenos excessos de Ni em fadiga de baixo ciclo por meio de uma avaliação do efeito de tratamentos térmicos de recozimento realizados em diferentes temperaturas na vida em fadiga, associando estes efeitos à constituição de fases determinada. Adicionalmente, a influência da amplitude de deformação e da temperatura de ensaio foram avaliadas separadamente.

INTRODUCTION

Shape memory effect (SME) is defined as the capability that some materials present to recover their original shape after an apparently permanent deformation through proper stimulus. Superelasticity (SE) is a specific shape memory effect case where the strained structure recovers its shape simply by unloading. Through a proper selection of chemical composition and suitable heat treatments, a shape memory alloy can present one effect or the other in determined work conditions (1).

Both of these effects are related to a thermoelastic martensitic transformation involving a high temperature austenitic phase and a low temperature martensitic phase. Martensitic transformations (MT) are diffusionless, athermic, shear transformations that involve cooperative and simultaneous movement of several atoms through distances smaller than the interatomic during continuous cooling. This transformation begins when the austenitic component's temperature is lowered to a critical temperature named Ms, associated with the network shearing driving force.

The transformation continuous through cooling and the structure becomes completely martensitic when the ending transformation temperature Mf is reached. If the cooling is interrupted between Ms and Mf, the transformation will cease and a two-phase austenitic + martenstic structure will be achieved. Inside of an austenitic grain, the martensite formed during a free of tension cooling, named thermal martensite, may be formed in several different orientations, each orientation corresponding to a martensite variant.

During heating, the reverse transformation (RT) from martensite to austenite occurs, beginning in the critical temperature As and ending at the critical temperature Af. Therefore, a thermal hysteresis can be observed in the transformation cycle, being related to the non-chemical forces involved in the MT due to the interface movement during the network shearing (2–5).

In the conventional shape memory effect, the original shape of a structure can be recovered after being apparently permanently deformed through proper stimulus. In this case, the strains are produced by a variant reorientation mechanism when stress is applied in the martensitic structure, inducing a preferential orientation in this phase, which is now named detwinned martensite. When the loading is interrupted, the

produced strained is maintained, occurring only elastic recuperation. When this structure is heated above Af, the formation of austenite during the RT is accompanied by the recovery of the original shape. During cooling, the thermic martensite will be formed with variants in various orientations, resuming the original state (6).

In the superelasticity, on the other hand, when applying certain critical levels of stress (σ^{Ms}) in an initially austenitic structure, the martensite formation is induced by tension and with the induced transformation, a macroscopical deformation is produced. When the stress is removed, the martensite becomes unstable, the reverse transformation takes place and the initial shape is recovered. The result of these transformations induced during loading and unloading is that the material is able to recover from large strains simply by unloading (7,8).

However, it is worth noting that the martensitic transformation induced by tension occurs only in temperatures lower than a critical temperature Md. Since the austenite becomes more stable with increasing temperature, the tension required to induce martensite increases with increasing temperature. Thereby, in high enough temperatures, above Md, the driving force to induce martensite is so high that the austenite will deform plastically before σ^{Ms} is reached. On the other hand, in temperatures lower than As, the induced martensite will be stable even after withdrawing the tension, not recovering the shape during unloading (9).

Near equiatomic NiTi alloys are the most commercially used shape memory alloys. These alloys, which present a B2 cubic crystalline structure austenite and a B19' monoclinic martensite, exhibit low elastic anisotropy, low elastic modulus, biocompatibility and corrosion resistance. Due to their mechanical properties associated with their function SME and SE properties, they can be used in the actuator, sensors, coupling, medical and dental industries (7,10–12).

In the dental industry, the usage of NiTi became usual in the confection of orthodontic wires and endodontic files, mainly due to their great flexibility and low springback obtained due to their low stiffness, SME and SE. Thanks to these properties, NiTi files are capable of keeping the original root canal and even work in rotatory movements, providing higher efficiency to the endodontic treatments. (13–15).

However, despite of the favorable characteristics of these alloys, NiTi endodontic files can fracture by fatigue due to their rotatory movement. A fatigue fracture occurs with no previous macroscopic plastic deformation in such a way that the file can fracture unexpectedly during the procedure, with no previous mechanical waring. The file fracture inside of the root canal is a chirurgical complication that can compromise the result of the treatment when the extraction of the files' fragments is not viable (16–18).

In studies available in the literature, it is possible to notice that the fatigue resistance of NiTi files and wires is influenced by the present phases (12,16,19,20), by the presence of precipitates (21) and by the state of hardening (22) of the alloy. Other factors such as test temperature (23), file design (14) and the root canal geometrical characteristics (15) are also relevant.

In the manufacturing of NiTi endodontic, the continuous progress in heat-treatments performed in wires from which they are produced and/or in the files themselves as well as in the instruments design leads to the to improvements in flexibility and fatigue resistance in high deformation amplitudes, two essential properties during clinical application, as noted by several authors (12,24–26). While the instrument's design affects the maximum tension achieved in different regions of the file (27), heat-treatments determinate the microstructure and the microstructural state in the work temperature (25,28–30).

Thermomechanical treatments, as well as aging heat treatments, are successfully used in controlling the direct and reverse martensitic transformation temperatures in near-equiatomic Ni-rich NiTi alloys. These treatments favor the formation of three different precipitate phases, depending on the heat-treatment temperature and time, in the following precipitation sequence: Ti_3Ni_4, Ti_2Ni_3 and $TiNi_3$. The formation of theses precipitates is accompanied by a decrease in the Ni content of the austenitic matrix, which stabilizes according to the equilibrium between these two phases in certain temperatures. However, the transformation temperature is highly sensitive to the austenitic matrix chemical composition and the decrease of the Ni content in the austenite leads to an increase in the martensitic transformation start temperature, Ms, favoring it during cooling. In this manner, the heat treatment temperature determines the equilibrium chemical composition in the matrix and in the precipitate and, thus, the martensitic transformation temperature (7).

The presence of strain fields around the coherent intermediate Ti_3Ni_4 precipitates, on the other hand, favors the formation of the R-phase, a pre-martensitic trigonal phase. In these cases, the martensitic transformation occurs in two stages and the R-phase, which is the intermediate phase, can be obtained in suitable work temperatures. Thereby, Ti_3Ni_4 precipitates have also an important role on determining the transformation behavior and the microstructural evolution in these alloys. The B2 austenite → R-phase transformation also have a martensitic nature and the two-step MT B2 austenite → R-phase → B19' martensite is associated with lower lattice deformation in each step than the direct B2 austenite → B19' martensite transformation, (22,31–33).

In this manner, aging and thermomechanical treatments influence directly in the present phases in the work temperature and their stability by means of changes on the transformation sequence and critical temperatures and on the microstructure thermomechanical state, being determinant in controlling mechanical and functional properties (7). Studies performed in endodontic files indicate that the presence of the R-phase and martensite in heat-treated instruments is beneficial to improvements on the low cycle fatigue life when compared to the traditional superelastic instruments However, the relationship between these improvements resistance and the microstructure obtained during the performed treatments is not yet clearly understood since there are several parameters simultaneously involved and due to the significant role of the plastic deformation history (29,34).

In this context, this study has as main goal to elucidate the metallurgical and mechanical behavior of near equiatomic Ni-rich NiTi wires in low-cycle fatigue by means of an evaluation of the effect of annealing heat-treatments performed in different temperatures in the fatigue life, relating these effects to the microstructure inferred by the characterization analysis. Additionally, the influence of the strain amplitude and the fatigue test temperature were evaluated separately.

Referências Bibliográficas

1. Otsuka K, Wayman CM. Shape Memory Materials. Cambridge. Cambridge University Press; 1998. 284 p.

2. Krauss G. Steels - Processing, Structure, and Performance. Materials Park, Ohio: ASM International; 2005.

3. Reed-Hill RE. Physical Metallurgy Principles. 2nd ed. Nova York: D. Van Nostrand Company; 1973. 920 p.

4. Digges TG, Rosenberg SJ, Geil GW. Heat Treatment and Properties of Iron and Steel. National Bureau of Standards; 1966. 46 p.

5. Kato H, Yasuda Y, Sasaki K. Thermodynamic assessment of the stabilization effect in deformed shape memory alloy martensite. Acta Mater [Internet]. Acta Materialia Inc.; 2011;59(10):3955–64. Available from: http://dx.doi.org/10.1016/j.actamat.2011.03.021

6. Meyers MA, Chawla KK. Mechanical Behavior of Materials [Internet]. 2nd ed. Cambridge University Press; 2009. 882 p. Available from: http://www.smesfair.com/pdf/mechanical eng/smesfair09.pdf

7. Otsuka K, Ren X. Physical metallurgy of Ti – Ni-based shape memory alloys. Prog Mater Sci. 2005;50:511–678.

8. Wilkes KE, Liaw PK. The Fatigue Behavior of Shape-Memory Alloys. Jom. 2000;52(10):45–51.

9. WAYMAN, C.M.; DUERIG TW. An introduction to martensite and shape memory. Engineering Aspects of Shape Memory Alloys. London: Butterworth-Heinemann, London; 1990. p. 1990.

10. Feninat F El, Laroche G, Fiset M, Mantovani D. Shape Memory Materials for Biomedical Applications. Adv Eng Mater. 2002;4(3):91–104.

11. Yahata Y, Yoneyama T, Hayashi Y, Ebihara A, Doi H, Hanawa T, et al. Effect of heat treatment on transformation temperatures and bending properties of nickel – titanium endodontic instruments. Int Endod J. 2009;42:621–6.

12. Shen Y, Zhou H, Zheng Y, Peng B, Haapasalo M. Current Challenges and Concepts of the Thermomechanical Treatment of Nickel-Titanium Instruments. J Endod [Internet]. Elsevier Ltd; 2013;39(2):163–72. Available from: http://dx.doi.org/10.1016/j.joen.2012.11.005

13. Sattapan B, Nervo GJ, Palamara JEA, Messer HH. Defects in Rotary Nickel-Titanium Files After Clinical Use. J Endod. 2000;26(3):161–5.

14. Melo MCC de, Bahia MG de A, Buono VTL. Fatigue resistance of engine-driven rotary nickel-titanium endodontic instruments. J Endod. 2002;28(11):765–9.

15. Chi C, Li C, Lin C, Shin C. Cyclic fatigue behavior of nickel-titanium dental rotary files in clinical simulated root canals. J Formos Med Assoc [Internet]. Elsevier Ltd; 2017;116(4):306–12. Available from: http://dx.doi.org/10.1016/j.jfma.2016.06.002

16. Braga LCM, Silva ACF, Buono VTL, Bahia MG de A. Impact of Heat Treatments on the Fatigue Resistance of Different Rotary Nickel-titanium Instruments. J Endod. 2014;40(9):7–10.

17. Bahia MGA, Martins RC, Gonzalez BM, Buono VTL. Physical and mechanical characterization and the influence of cyclic loading on the behaviour of nickel-titanium wires employed in the manufacture of rotary endodontic instruments. Int Endod J. 2005;38:795–801.

18. Carvalho A, Montalvão D, Freitas M, Reis L, Fonte M. Determination of the rotary fatigue life of NiTi alloy wires. Theor Appl Fract Mech. 2016;85:37–44.

19. Figueiredo AM, Modenesi P, Buono V. Low-cycle fatigue life of superelastic NiTi wires. Int J Fatigue [Internet]. Elsevier Ltd; 2009;31(4):751–8. Available from: http://dx.doi.org/10.1016/j.ijfatigue.2008.03.014

20. Pelton AR. Nitinol Fatigue : A Review of Microstructures and Mechanisms. J Mater Eng Perform. 2011;20(July):613–7.

21. Gall K, Maier HJ. Cyclic deformation mechanisms in precipitated NiTi shape memory alloys. Acta Mater. 2002;50:4643–57.

22. Kuhn G, Jordan L. Fatigue and Mechanical Properties of Nickel- Titanium

Endodontic Instruments. J Endod. 2002;28(10):716–20.

23. Nemat-nasser S, Guo W-G. Superelastic and cyclic response of NiTi SMA at various strain rates and temperatures. Mech Mater. 2006;38:463–74.

24. Parashos P, Messer HH. Rotary NiTi Instrument Fracture and its Consequences. J Endod. 2006;32(11):30–4.

25. Shen Y, Qian W, Abtin H, Gao Y, Haapasalo M. Fatigue testing of controlled memory wire nickel-titanium rotary instruments. J Endod [Internet]. Elsevier Ltd; 2011;37(7):997–1001. Available from: http://dx.doi.org/10.1016/j.joen.2011.03.023

26. Lopes HP, Gambarra-Soares T, Elias CN, Siqueira JF, Inojosa IFJ, Lopes WSP, et al. Comparison of the mechanical properties of rotary instruments made of conventional nickel-titanium wire, M-Wire, or nickel-titanium alloy in R-phase. J Endod. 2013;39(4):516–20.

27. Santos L de A, López JB, Las Casas EB de, Bahia MG de A, Buono VTL. Mechanical behavior of three nickel-titanium rotary fi les : A comparison of numerical simulation with bending and torsion tests. Mater Sci Eng C [Internet]. Elsevier B.V.; 2014;37:258–63. Available from: http://dx.doi.org/10.1016/j.msec.2014.01.025

28. Pereira ESJ, Viana ACD, Buono VTL, Peters OA, Bahia MG de A. Behavior of Nickel-Titanium Instruments Manufactured with Different Thermal Treatments. J Endod. 2015;41(1):67–71.

29. Braga LCM, Silva ACF, Buono VTL, Bahia MG de A. Impact of Heat Treatments on the Fatigue Resistance of Different Rotary Nickel-titanium Instruments. J Endod. 2014;40(9):1494–7.

30. Pereira ESJ, Gomes RO, Leroy AMF, Singh R, Peters OA, Bahia MGA, et al. Mechanical behavior of M-Wire and conventional NiTi wire used to manufacture rotary endodontic instruments. Dent Mater. 2013;29:e318–24.

31. Khalil-Allafi J, Behnam A-A. Multiple-step martensitic transformations in the Ni 51 Ti 49 single. J Mater Sci. 2010;45:6440–5.

32. JIANG S, ZHAO Y, ZHANG Y, HU L, LIANG Y. Effect of solution treatment and aging on microstructural evolution and mechanical behavior of NiTi shape memory alloy. Trans Nonferrous Met Soc China [Internet]. 2013;23(12):3658–67. Available from: http://linkinghub.elsevier.com/retrieve/pii/S1003632613629143

33. Jiang F, Liu Y, Yang H, Li L, Zheng Y. Effect of ageing treatment on the deformation behaviour of Ti – 50 . 9 at .% Ni. Acta Mater [Internet]. Acta Materialia Inc.; 2009;57(16):4773–81. Available from: http://dx.doi.org/10.1016/j.actamat.2009.06.059

34. Liu Y, Humbeeck J Van, Stalmans R, Delaey L. Some aspects of the properties of NiTi shape memory alloy. J Alloys Compd. 1997;247:115–21.

2. OBJETIVOS

2.1. Objetivo Geral

O objetivo geral deste trabalho foi avaliar a influência de tratamentos térmicos na constituição e nas propriedades mecânicas de fios de NiTi inicialmente superelásticos, visando a melhoria de sua resistência à fadiga e um melhor entendimento dos mecanismos.

2.2. Objetivos Específicos

Realizar tratamentos térmicos de envelhecimento nos fios de NiTi visando obter diferentes microestruturas após resfriamento até a temperatura ambiente;

Avaliar o comportamento do material tratado em ensaios de fadiga com elevada amplitude de deformação.

Avaliar a influência da amplitude de deformação na resistência à fadiga dos fios tratados termicamente.

Avaliar o comportamento mecânico em tração de fios tratados termicamente.

Avaliar a influência da temperatura de ensaio na resistência à fadiga do material estudado.

Avaliar a influência das fases presentes na microestrutra na resistência à fadiga de fios tratados termicamente.

ESTRUTURA DA DISSERTAÇÃO

No primeiro tópico desta dissertação, foi feita uma breve contextualização do assunto a ser abordado e no segundo, foram apresentados os objetivos desta dissertação. Nos tópicos seguintes, a metodologia experimental e os resultados serão abordados nos artigos produzidos durante o desenvolvimento deste trabalho, que serão apresentados na seguinte ordem:

1 - Effects of Aging Treatments on the Fatigue Resistance of Superelastic NiTi Wires (Submetido para publicação no periódico Materials Science and Engineering A);

2 - Fatigue Resistance at Different Maximum Strain Amplitudes of Dual-Phase NiTi Wires (Submetido para publicação no periódico International Journal of Fatigue);

3 - The Effect of Low-Temperature Heat-Treatment on the Tensile and Fatigue Behavior of an Initially Superelastic NiTi Wire (Apresentado no Congresso Brasileiro de Engenharia e Ciência dos Materiais e submetido para publicação no periódico Materials Research)

4 - Effect of Phase Constitution in Low-Cycle Fatigue of NiTi Wires (A ser submetido)

No artigo 1, são apresentados os resultados de tratamentos térmicos realizados em diferentes temperaturas e sua influência na resistência à fadiga sob uma amplitude de deformação de 4% a 37°C. As condições de tratamento que apresentaram melhor comportamento em fadiga foram utilizadas para avaliar a influência da amplitude de deformação nessa propriedade no artigo 2. No artigo 3, ensaios a 4% de deformação foram realizados também a 25°C em fios tratados a 400°C, permitindo-se uma comparação com os ensaios realizados a 37°C para uma avaliação da influência da temperatura de ensaio na resistência à fadiga em temperaturas nas quais a microestrutura esperada foi mantida. Uma análise do comportamento em tração destes fios também foi realizada. Por fim, fixou-se uma condição de tratamento térmico e a vida em fadiga foi avaliada em diferentes temperaturas de ensaio, desta vez, escolhidas

de forma a se obter diferentes microestruturas iniciais nos ensaios, conforme detalhado no artigo 4.

3. EFFECTS OF AGING TREATMENTS ON THE FATIGUE RESISTANCE OF SUPERELASTIC NiTi WIRES

Jéssica Dornelas Silva*, Pedro Damas Resende, Suzanny Cristina Martins, Bárbara Moreno Pagotto, Natalia Isabel de Azevedo Lopes, Leandro de Arruda Santos, Vicente Tadeu Lopes Buono

Department of Metallurgical and Materials Engineering, Universidade Federal de Minas Gerais (UFMG), Belo Horizonte, MG, Brazil

*Corresponding author: jdornelas.ufop@gmail.com

Abstract

Aging treatments can be powerful tools to improve the fatigue life of NiTi wires submitted to severe conditions of cyclic deformation. In this work, aging treatments were performed in an initially superelastic NiTi wire in temperatures ranging from 300^{o}C until 600^{o}C for 30 min. The as-received and heat-treated wires' microstructures were characterized by XRD, the transformation temperatures were obtained by DSC and the mechanical characterization was performed via tensile tests. The wires were then submitted to low-cycle fatigue tests in a rotating-bending machine at a maximum strain of 4%. The heat treatments were effective on improving the fatigue resistance, especially when the R-phase was formed. The highest number of cycles to failure was obtained in the samples heat treated at 400 ^{o}C and 450 ^{o}C.

Keywords: nickel-titanium alloys, shape memory, aging, low-cycle fatigue

3.1. Introduction

Near equiatomic NiTi alloys are smart materials known by their capability of recovering large strains as a result of a thermoelastic martensitic transformation involving a high temperature austenitic B2 phase and a low-temperature martensitic B19' phase. When the alloy is deformed in the martensitic phase and the shape recovery is achieved upon heating above a critical temperature, the shape memory effect (SME) is said to take place. When the austenite is deformed and the shape is recovered simply by unloading, the effect is called pseudoelasticity or superelasticity (SE) (1).

NiTi's functional properties combined with a high corrosion resistance and biocompatibility make them suitable to a wide range of engineering and medical applications, such as sensors and actuators, joining devices, cardiovascular stents, orthodontic wires, endodontic files, and orthopedic components. In many of these applications, NiTi wires are subjected to fluctuating loads or strains, making fatigue resistance relevant to the material's development (2–5).

Thermomechanical and aging treatments are successfully used to control the martensitic transformation temperatures of near-equiatomic, Ni-rich NiTi alloys through the precipitation of Ni-rich particles. The precipitation of coherent Ti_3Ni_4 particles that can occur during these treatments induces the formation of a rhombohedral pre-martensitic phase, known as the R-phase, resulting in a multi-stage transformation. The mechanical properties obtained from changes in the microstructure caused by thermomechanical and aging treatments can be useful as a powerful tool to improve the fatigue resistance of NiTi alloys (1,6–8).

Previous studies have shown that the low-cycle fatigue life of an austenitic NiTi structure can in fact be improved through appropriate heat treatments (2,9). However, the mechanisms of these fatigue improvements are not yet clearly understood. In this context, this study aims to perform heat treatments in a wide range of temperatures in an initially superelastic NiTi wire and evaluate the fatigue resistance of the resultant microstructure when subjected to an aggressive strain-controlled condition.

3.2. Experimental procedure

An annealed and pickled 1mm diameter NiTi wire was used in this study. In the as-received (AR) condition, the wire presented an austenitic superelastic microstructure and a nominal atomic composition of 51%Ni-49%Ti.

The heat treatments were performed on 12 cm long samples cut off from the AR wire in a tubular furnace with an argon controlled-atmosphere for 30 min and then water cooled. The following temperatures were employed: 300°C, 350°C, 400°C, 450°C, 500°C, 550°C and 600°C. The samples were identified according to the treatment temperatures as S300, S350, S400, S450, S500, S550 and S600 respectively.

For microstructural investigation, samples of 1 cm in length were cut from the heat treated samples and analyzed by X-ray diffraction (XRD) in a PANalytical PW1710

diffractometer. The tests were performed with 2θ ranging from 30° to 120° using Cu-Kα radiation and a scan speed of 0.02°/s. Diffraction patterns available in the literature and in the ICSD database were used to identify the observed peaks.

The martensitic direct (Ms, Mf) and reverse (As, Af) transformation temperatures were determined by differential scanning calorimetry (DSC) in a Shimadzu DSC-60 calorimeter at a cooling/heating rate of 10°C/min. The tests were performed in triplicate by cooling each specimen from room temperature to -100°C, following by heating to 100°C, cooling it back to -100°C and heating to room temperature. The reverse transformation temperatures were determined in the interval from -100°C to 100°C, while the direct ones on the subsequent cooling step.

For mechanical evaluation, tensile tests were carried out according to ASTM F2516 − 14 (10) in an Instron 5582 testing machine. Loading until rupture was performed at a crosshead speed of 12 mm/min. Tests of loading up to 6% total strain and unloading at a crosshead speed of 1.2 mm/min were also performed. The experiments were repeated three times.

Finally, bending-rotating fatigue tests were performed on proper equipment in a water bath at 37°C at a fixed maximum strain of 4% and a statistical analysis was made in order to acquire the mean number of cycles to failure. The fractured surfaces were analyzed in Secondary Electron Images (SEI) recorded in a FEI – Inspect F50 scanning electron microscope (SEM) operating at 15 kV.

3.3. Results

3.3.1. X-ray diffraction

Figure 1 shows the XRD peaks obtained from the AR and the heat-treated samples. The austenitic phase is easily identified in the AR as well as in S300 and S350. Samples treated at 400°C and 450°C showed the presence of the R-phase, characterized by the splitting of the $(100)_{B2}$ peak showed in Figure 1(b) (11). The diffractogram of S500 indicates that a transitioning structure constituted by the R-phase and some amount of austenite was developed. Austenite becomes the predominant phase again at S550 and at S600. Ti_3Ni_4 peaks can be observed at S500, S550 and S600, indicated by empty arrows in Figure 1(a), while Ti_2Ni_3 peaks are present at S600, indicated by filled arrows, as also observed by Srivastava et al., 2008 (12).

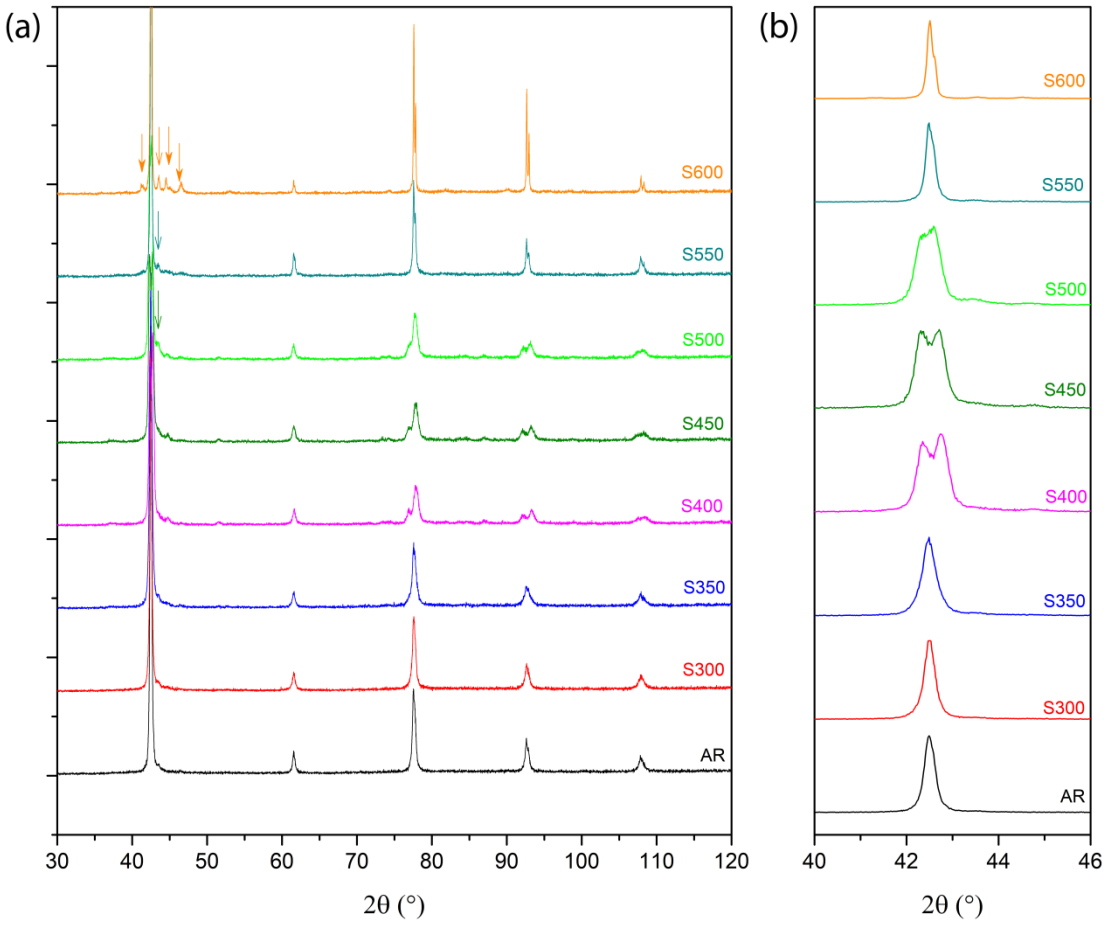

Figure 3.1 – (a)XRD spectra at room temperature for the as-received and the heat-treated samples and (b) (100)B2 peak and peak splitting for the R-phase.

3.3.2. Differential Scanning Calorimetry – DSC

The DSC charts are presented in Figure 2. AR, S300 and S350 presented smooth B2 → B19' transformation peaks during cooling and B19' → B2 during heating. The B19' → B2 heating peak in S350 presents a small split, indicating that there are actually two overlapping peaks.

The sample treated at 400°C, on the other hand, presented a sharp cooling peak and two well-defined heating peaks. The profile of the cooling peak is typical of a B2 → R transformation (11), in agreement with the XRD results. The first and broader heating peak is related to a B19'→ R transformation, which indicates that the R-phase → B19' transformation occurred during cooling even though its peak was not detected. In fact, it has been previously reported (13,14) that the R → B19' peak is of difficult detection due to its flatness and also because it can be an incomplete peak around the lower

temperature limit, in a region indicated by the arrow in the S400 chart. The second and sharper heating peak refers to an R → B2 transformation.

Accordingly, the R → B19’ peak can be seen on the DSC charts of S450 and S500 as flat peaks at low temperatures at the end of the cooling curves. These two samples also presented the B2 → R peaks during cooling and the two-step B19’ → R → B2 transformation during heating. As follows, at S400, S450, and S500, symmetric R-phase transformations (14) were observed.

The samples treated at 550°C, on the other hand, presented well defined B2 → R and R → B19’ peaks during cooling and one direct B19’ → B2 transformation peak during heating in an asymmetric R-phase transformation. Samples treated at 600°C, exhibited direct phase transformation peaks both on cooling (B2 → B19’) and on heating (B19’ → B2).

Table 1 presents the mean transformation temperatures for each heat treatment with standard deviation lower than 2%. Ms and Mf refer, respectively, to the martensitic start and finishing transformation temperatures (B2 → B19’ or R → B19’) and Rs and Rf refer to the R-phase transformation start and finishing temperatures (B2 → R) during cooling while R’s and R’f refer, respectively, to the R-phase transformation (B19’ → R) start and finishing temperatures and As and Af refer to the austenitic start and finishing temperatures (B19’ → B2 or R → B2) during heating.

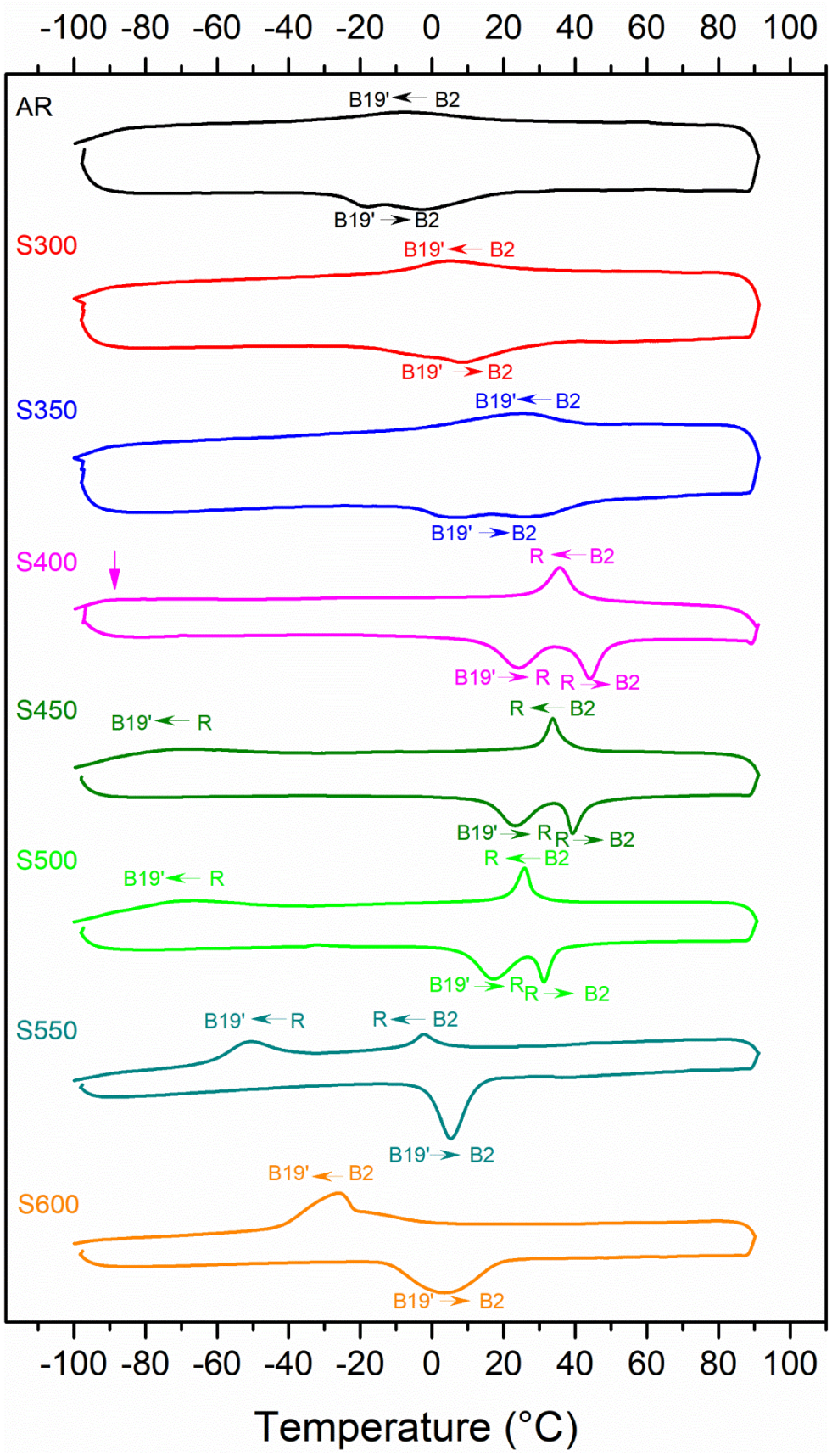

Figure 3.2 – Representative DSC curves.

Table 3.1 – Mean transformation temperatures obtained from the DSC charts**.**

	R's (°C)	R'f (°C)	As (°C)	Af (°C)	Rs (°C)	Rf (°C)	Ms (°C)	Mf (°C)
AR	--	--	-29	19	--	--	19	-38
S300	--	--	-5	21	--	--	20	-11
S350	--	--	-5	38	--	--	38	-2
S400	16	31	39	49	43	32	--	--
S450	17	31	37	44	38	31	-46	-85
S500	11	25	30	35	29	23	-46	-81
S550	--	--	0	12	3	-5	-41	-57
S600	--	--	-11	19	--	--	-19	-41

3.3.3. Tensile Tests

On the tensile stress vs tensile strain curves (Figure 3), it can be seen that the AR, S300, and S350 exhibited superelasticity, as expected for an austenitic structure, while S550 and S600 did not, even though they exhibited austenitic structure. On the other hand, S400, S450, and S500, constituted mainly by the R-phase, presented basically only elastic recovery after cycling but a full shape recovery could be achieved by heating.

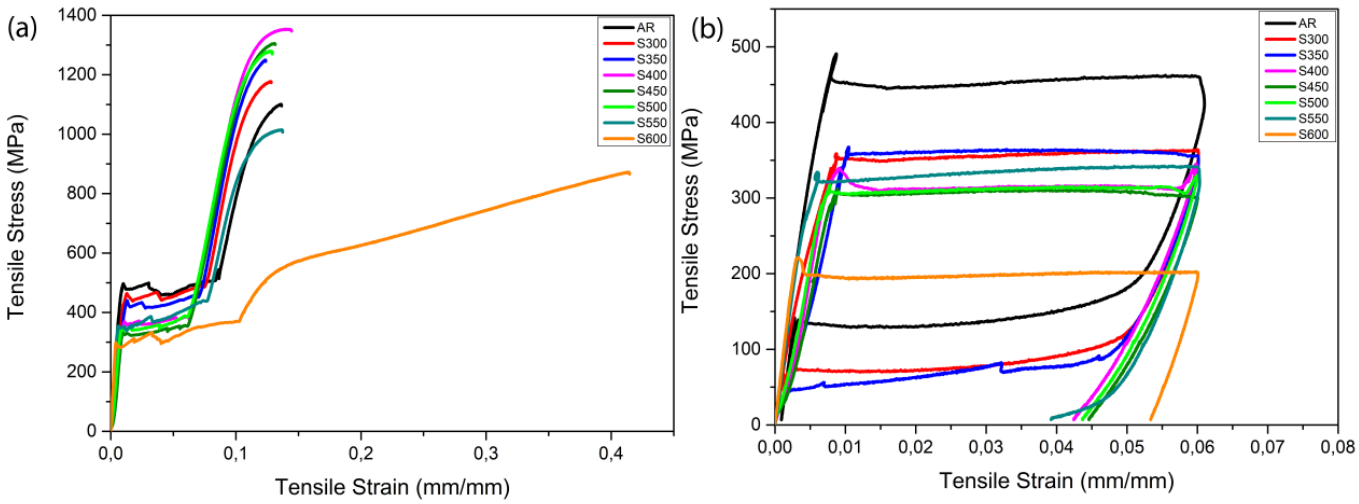

Figure 3.3 – Representative stress strain (a) rupture curves and (b) cyclic curves obtained during tensile tests at room temperature**.**

Table 2 presents the apparent elastic moduli (Ea) and the stress required to initiate the martensitic transformation plateau (σ_{MI}) obtained from the cycling curves. The average ultimate tensile strength (σ_u), obtained from the rupture curves, is also shown in the table. The maximum standard deviation obtained was 6%.

Table 3.2 – Mean values of aparent modulus of elasticity (Ea), stress required to induce the martensitic transformation (σ_{MI}) and ultimante tensile strength (σ_u) obtained from the stress vs strain curves.

	Ea (GPa)	**σ_{MI} (MPa)**	**σ_u (MPa)**
AR	66	444	1093
S300	42	352	1145
S350	36	359	1247
S400	48	307	1349
S450	44	304	1306
S500	48	307	1281
S550	63	313	1006
S600	76	194	873.0

3.3.4. Fatigue Life

The mean number of cycles to failure in each condition is presented on the graph in Figure 4. It is possible to see that the heat treatments were effective on improving the fatigue life of the AR wire. The higher fatigue resistance was obtained at S450.

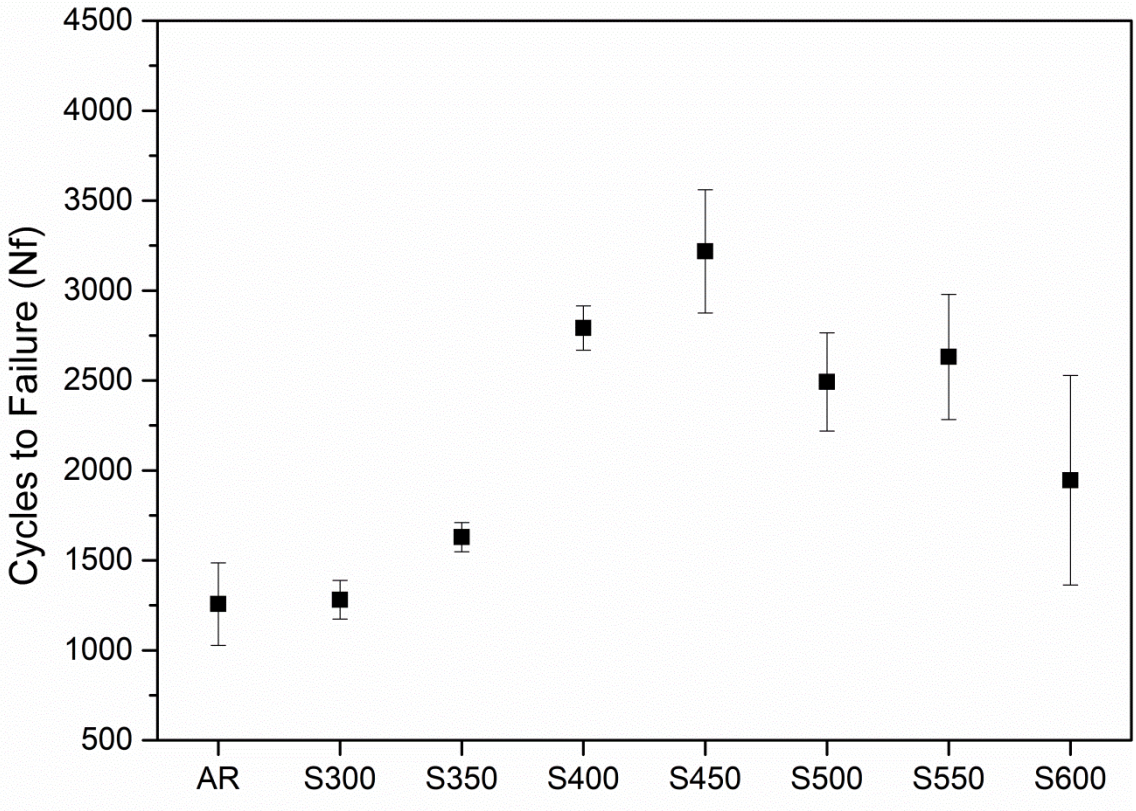

Figure 3.4 – Mean number of cycles to failure for the as-received and the heat treated samples at 4% maximum strain.

The fracture surfaces presented two different morphological regions: a region of slow crack nucleation and propagation, called the fatigue region, and a final ductile rupture region. Figure 5 illustrates these two regions in S300 and S450. The fatigue regions are characterized by striations while the ductile region is characterized by the presence of dimples or microvoids. In S450, the fatigue striations spacing is small and the dimples are finer, while S300 presents cracks on the fatigue surface.

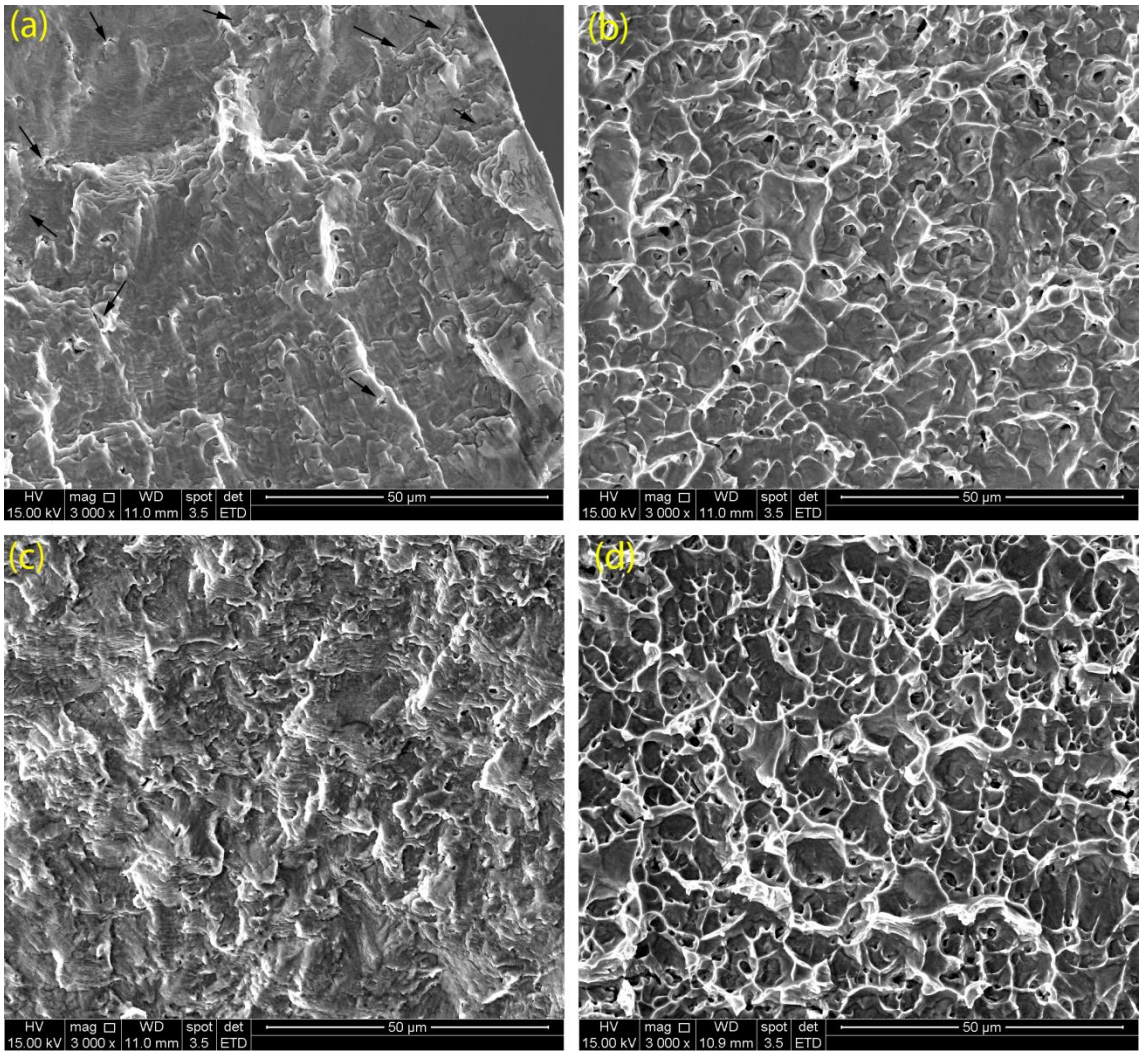

Figure 3.5 – Fracture surfaces for (a) and (b) S300 and (c) and (d) S450.

3.4. Discussion

3.4.1. Recovery processes

Both the flat transformations peaks on the DSC chart and the high stress required to induce the transformation plateau (σ_{MI}) indicate that the AR sample is constituted by a hardened structure with a high density of dislocations and heterogeneities. During the performed heat treatments, dislocations move, reorganize and annihilate each other, resulting in structures with different thermomechanical states. In the austenitic wires, the annealing process can be directly related to the value of the stress plateau: according to Otsuka and Ren, 2005 (1), a high density of dislocations, such as in AR, offers resistance to the lattice distortions required by the martensitic transformation, while rearranged dislocation structures contribute to a smooth transformation. During the 300

°C and 350 °C heat treatments, the AR sample undergoes recovery, where the initially tangled dislocations rearrange into dislocation cells. The martensitic transformation occurs easily on recovered structures, resulting in a decrease in σ_{MI} and, also, an increase in Ms and Mf, as shown in Table 1. The increase in the martensitic transformation temperature is larger the further is the recovery achieved.

The σ_{MI} stress decreases after heat treating at 550°C and at 600°C and there is a decrease in Ms and Mf. These effects indicate that these samples are in a stage of low dislocation density as compared to the AR, S300 and S350 samples, in which the dislocation networks assist the martensitic transformation by offering stress fields to decrease the required undercooling. The existence of a dislocation structure itself means that the stresses involved in the transformation are higher when compared to structures with a high degree of recovery. In such case, it is reasonable to assume that S550 is in a highly recovered stage, with a low density of dislocations, and S600, which suffered a large drop in σ_{MI}, went through recrystallization. The recrystallization of the S600 sample becomes clear on the rupture curve, where it presents a low ultimate tensile strength and a high ductility when compared to all of the other samples. Also, the well-defined direct transformation DSC peaks can be associated with a homogenous structure, with a low density of defects.

The association between the stress plateau and the recuperation process cannot be made on the R-phase wires since the effect of the dislocation structure becomes very small for a transformation that involves small lattice distortions like the R-phase transformation (15,16). In this case, the transformation plateau becomes less dependent on the thermomechanical state of the initial structure and the different R-phase samples present similar σ_{MI}. In these samples, the formation of the intermediate Ti_3Ni_4 phase as fine and coherent precipitates is relevant, as it will be discussed below.

3.4.2. Precipitation reactions

As discussed in the literature (1,17), the formation of Ni-rich precipitates on heat treated samples is accompanied by different effects:

- Increase on the martensitic transformation temperatures due to the Ni-content depletion on the matrix;
- R-phase formation and, hence, two-step transformation;

- Precipitation hardening.

In this manner, the precipitation state of the samples can be inferred from the tensile strength, the presence of a phase transformation involving the R-phase on the DSC charts and the transformations temperatures.

From the rupture curves in Figure 3 and the ultimate tensile strength (σ_u) presented in Table 2, the tensile strength changes from higher to lower values in the following sequence: S400, S450, S500, S350, S300, AR, S550, and S600. Well defined R-phase transformation peaks on the DSC charts of samples S400, S450 and S500 were observed in Fig. 1, indicating that precipitation of coherent Ti_3Ni_4 particles took place within this temperature range. Analyzing the mean transformation temperatures in Table 1, it can be seen that Mf increased with increasing temperature, indicating that the higher the temperature, the larger the fraction of precipitates formed and more Ni is removed from the matrix. The decrease in the tensile strength from S400 to S500 is evidence that at S400 there is a dispersion of fine precipitates, while at S450 and S500, there is precipitation growth rather than the nucleation of new fine precipitates.

In S350, some precipitation probably occurred, enough to increase the σ_u when compared to S300 and AR and to initiate two-step transformation involving the R-phase as observed in the peak splitting in the DSC charts in Figure 2.

In S550, the occurrence of the precipitation of coherent Ti_3Ni_4 is also evidenced by the occurrence of the R-phase transformation. But these precipitates did not harden the structure anymore and, actually, the low density of dislocation resultant from the recovery process becomes relevant and a decrease in σ_u can be observed when S550 is compared to AR**.** This means that amount of the precipitates have grown, and thus they could be detected on the XRD analysis, and that their size increased, they are about to lose coherency.

At last, when comparing S600 to S400, S450, S500, and S550, suppression of the R-phase transformation followed by an increase in Ms and Mf could be observed. The increases on the transformation temperatures suggest that precipitation continued to occur. But, on S600, like on S550, the precipitation did not harden the structure. This is an indication that overaging is taking place and the precipitates are no longer coherent with the matrix, affecting only the transformation temperatures by decreasing the Ni-

content of the matrix. These results are in accordance with the Ti_2Ni_3 peaks observed in the S600 XRD spectrum.

3.4.3. Microstructure development

Considering the characterization results obtained in this study, it is possible to establish the microstructural constitution and thermomechanical state of the analyzed wires at room temperature:

- AR: an austenitic superelastic wire, characterized by a high density of dislocations and defects;
- S300: a recovered austenitic superelastic wire, with rearranged dislocations;
- S350: a recovered austenitic superelastic wire, with rearranged dislocations;
- S400: R-phase structure with fine and dispersive Ti_3Ni_4 coherent precipitates;
- S450: R-phase structure with fine and dispersive Ti_3Ni_4 coherent precipitates;
- S500: R-phase + austenitic structure with Ti_3Ni_4 coherent precipitates;
- S550: a recovered austenitic structure with large Ti_3Ni_4 precipitates;
- S600: a recrystallized austenitic structure with Ti_2Ni_3 precipitates.

3.4.4. Deformation behavior

The deformation behavior, analyzed by means of the tensile tests at room temperature, allows the following interpretations.

At AR, S300, S350, S550, and S600, austenite deforms elastically until σ_{MI} is reached and oriented martensite starts to be induced by stress. When the induced transformation is complete, martensite starts to deform elastically, plastically and, then, the wire finally ruptures. AR, S300, S350, and S550, present a tendency towards brittle behavior, with only small amounts of plastic deformation observed. S600, on the other hand, undergoes strain hardening and a large plastic strain.

At these samples' cyclic curves, AR, S300, S350 recover from the previous deformation during unloading, while those treated from 400°C to 600°C show residual strains after unloading. S550 and S600 also showed low values of σ_u and despite the low stress required to induce the martensitic transformation in these samples, the occurrence of plastic deformation suppresses the shape recovery, resulting in the loss of the functional properties.

The apparent elastic modulus (Ea) and the stress required to induce martensite (σ_{MI}) vary from one sample to another, being deeply related to the thermomechanical state of the microstructure, involving the presence of dislocation, how they are organized and the presence of precipitates. The effect of the recovery process on σ_{MI} has been previously discussed on topic 4.1, but this process can also be related to the observed decrease on Ea at S300 and S350 comparing to AR. On the treated samples, the dislocation cells created by the recovery process promote the nucleation of stress-induced martensite. The formation of localized martensite nuclei generates instabilities on the austenite's elastic deformation region, resulting in a lower apparent modulus. At S550 and S600, on the other hand, the observed Ea are as high as expected for the austenitic microstructure. Probably, at S550 the dislocation cells are too large to have any influence in the induced martensitic transformation and at S600 recrystallization took place.

The samples treated at 400°C, 450°C, and 500°C, on the other hand, presented σ_{MI} with values very close to each other and lower than the non-recrystallized austenitic ones. That happens because this plateau represents the induced transformation of martensite from the R-phase rather than from austenite. Since this transformation involves much smaller lattice distortion than directly from austenite, it requires lower levels of stress and becomes less dependent on the thermomechanical state of the initial structure.

3.4.5. Fatigue mechanisms

To understand the improvement in fatigue resistance and the fatigue mechanisms, some aspects should be noted. First, low-cycle strain-controlled fatigue is reported to be controlled by crack propagation (2,9,18,19). In fact, the high flexural strain used on this study favors fast crack nucleation on regions of stress concentration such as on surface defects and around inclusions. In this manner, cracks nucleate easily, and the fatigue life is, in fact, controlled by crack propagation.

Secondly, three distinct fatigue mechanisms can be distinguished in this study. They depend on the microstructure at 37°C of the analyzed samples. There were the austenitic wires (AR, S300 and S350), the R-phase wires (S400 and S450) and the austenitic + precipitates wires (S500, S550, S600). The higher fatigue resistance was measured in S400 and S450, which presented the R-phase structure. The R-phase is a pre-martensitic phase that easily transforms into B19' martensite and, in the present condition, it does

not transforms back during cycling according to the tensile cycling curves, like observed by Santos, 2016(20). In this manner, B19' martensite should be the predominant phase on the 4% bending-rotating fatigue test, being the phase that bears most of the mechanical cycling. The martensite variants offer multiple paths for propagation of the nucleated cracks, a fact that promotes crack branching, which, in turn, leads to high energy dispersion as the process takes place (9). During cycling, the induced martensite variants undergo increasing reorientation until a point where they are so favorably orientated at the crack tip that branching no longer occurs and the wire ruptures rapidly. These assumptions are supported by the fracture surfaces. The fine striation spacing in S450 is related to a high number of cycles spent on the fatigue regime.

In superelastic NiTi, the stress concentration around the crack tip and the crack propagation itself are strongly influenced by the induced martensitic transformation rather than by a plastic region like in conventional materials. In fact, previous studies have shown that under cyclic loading, crack tip blunting does not occur in superelastic NiTi (3). Instead, they observed that stress-induced martensite forms in front of the crack tip, indicating that direct and reverse martensitic transformation probably occurs during cycling. Moreover, DELVILLE et al., 2011(21) observed that dislocation slip occurs alongside with the stress induced martensitic transformation during cycling initially superelastic NiTi. Accordinly, Alarcon et al., 2017(4) reported that the martensitic transformation actually assists the crack grownth when its critical size has been reached since the strains produced during this transformation provides additional driving force for the crack opening. HELLER et al., 2018 (22) observed that stress inducing martensite from austenite generates more defects than reorientation of martensite variants under stress. Thus, the higher defect accumulation involved in the martensitic induced transformation can explain the inferior low-cycle response of austenitic wires. The cracks observed on the fracture surface of S300 can be related to the defects generated during cycling. When the induced martensitic transformation occurs easily, reflected by a lower σ_{MI}, such as in S500 and S550, fewer defects are produced and a higher number of cycles to failure is observed.

Despite being constituted basically by R-phase at room temperature, S500 is completely austenitic at 37°C. This explains the drop in Nf and how similar its behavior is to S550, both being constituted by recovered austenite and larger Ti_3Ni_4 precipitates. Their

fatigue resistance is higher than AR, S300, and S350 due to the decrease in σ_{MI} and the less accumulated defects, following the initial trend for austenitic wires.

The presence of plastic deformation in this material can result in a complex behavior and apparently hinders the fatigue resistance and results in large dispersions in Nf, as observed for S550 and S600. On the recrystallized structures, the low σ_u indicates that a large amount of plastic deformation can occur microscopically during cycling and a decrease on the fatigue life can be observed.

In this way, to obtain an optimum fatigue resistance, it is necessary to balance a smooth martensite induced transformation and a high enough mechanical strength on austenitic wires. And, finally, the best way to achieve the higher fatigue life in the AR wire was to perform a heat treatment that produces a microstructure containing the R-phase with finely dispersed Ti3Ni4 precipitates.

3.5. Conclusions

In this paper, aging treatments were performed in initially superelastic NiTi wires and the effects of these heat-treatments on the microstructure and the fatigue resistance were evaluated. The microstructural state was analyzed by XRD and inferred by comparing the mechanical properties measured in tensile tests and the transformation temperatures obtained from the DSC measurements. The following observations were made:

- The heat-treatments at 300°C and 350°C promoted the recovery of the deformed austenite, while the treatments at 400°C and higher temperatures promoted the precipitation process. Initially, the Ti_3Ni_4 precipitates are fine and dispersed in the B2 matrix, but at higher temperatures, the amount and size of the precipitates increased, as shown by the decrease in ultimate tensile stress and the increase in transformation temperatures. The behavior of the samples treated at 600°C indicates that recrystallization occurred.
- Significant increases in the number of cycles to failure were observed when the heat treatment temperature increased until 450°C, suggesting that precipitation of fine and coherent Ti_3Ni_4 particles and of the R-phase had occurred. The highest fatigue resistance was obtained in the samples treated at 400°C and 450°C.
- Fatigue mechanisms in the austenitic and R-phase wires were proposed:

- During cycling, austenitic wires undergo direct and reverse martensitic transformation, but this induced transformation is accompanied by the accumulation of defects. In these wires, the fatigue resistance is higher when the martensitic transformation occurs easily in a high strength structure and, hence, is favored by the presence of dislocation cells and fine precipitates. Plastic deformation seems to harm the fatigue resistance.
- R-phase wires presented the higher number of cycles to failure due to crack branching on the induced martensitic structure. In these wires, the stress-induced B19' martensite is formed in the early stages of straining during the rotating bending fatigue test and the reverse transformation to R-phase does not occur. This martensite is reoriented during cycling until the point where the variants are favorably directed to the crack propagation and the wires suffer rapid final ductile failure.

Acknowledgements

This work was supported by Conselho Nacional de Desenvolvimento Científico e Tecnológico (CNPq), Coordenação de Aperfeiçoamento de Pessoal de Nível Superior (CAPES/PROEX) and the Fundação de Amparo à Pesquisa de Minas Gerais (FAPEMIG).

References

1. Otsuka K, Ren X. Physical metallurgy of Ti – Ni-based shape memory alloys. Prog Mater Sci. 2005;50:511–678.

2. Pelton AR. Nitinol Fatigue : A Review of Microstructures and Mechanisms. J Mater Eng Perform. 2011;20(July):613–7.

3. Di Cocco V, Iacoviello F, Maletta C, Natali S. Cyclic microstructural transitions and fracture micromechanisms in a near equiatomic NiTi alloy. Int J Fatigue [Internet]. Elsevier Ltd; 2014;58:136–43. Available from: http://dx.doi.org/10.1016/j.ijfatigue.2013.03.009

4. Alarcon E, Heller L, Chirani SA, Šittner P, Kopeček J, Saint-Sulpice L, et al. Fatigue performance of superelastic NiTi near stress-induced martensitic

transformation. Int J Fatigue. 2017;95:76–89.

5. Maletta C, Sgambitterra E, Furgiuele F, Casati R, Tuissi A. Fatigue of pseudoelastic NiTi within the stress-induced transformation regime: A modified Coffin-Manson approach. Smart Mater Struct. 2012;21(11).

6. Shen Y, Zhou H, Zheng Y, Peng B, Haapasalo M. Current Challenges and Concepts of the Thermomechanical Treatment of Nickel-Titanium Instruments. J Endod [Internet]. Elsevier Ltd; 2013;39(2):163–72. Available from: http://dx.doi.org/10.1016/j.joen.2012.11.005

7. Pereira ESJ, Viana ACD, Buono VTL, Peters OA, Bahia MG de A. Behavior of Nickel-Titanium Instruments Manufactured with Different Thermal Treatments. J Endod. 2015;41(1):67–71.

8. Gall K, Tyber J, Wilkesanders G, Robertson SW, Ritchie RO, Maier HJ. Effect of microstructure on the fatigue of hot-rolled and cold-drawn NiTi shape memory alloys. Mater Sci Eng A. 2008;486:389–403.

9. Figueiredo AM, Modenesi P, Buono V. Low-cycle fatigue life of superelastic NiTi wires. Int J Fatigue [Internet]. Elsevier Ltd; 2009;31(4):751–8. Available from: http://dx.doi.org/10.1016/j.ijfatigue.2008.03.014

10. Standard test method for tension testing of nickel-titanium superelastic materials. ASTM - F2516. 2015. p. 1–6.

11. Wang XB, Verlinden B, Van Humbeeck J. R-phase transformation in NiTi alloys. Mater Sci Technol [Internet]. 2014;30(13):1517–29. Available from: http://www.tandfonline.com/doi/full/10.1179/1743284714Y.0000000590

12. Srivastava AK, Yang Z, Schryvers D, Humbeeck J Van. Effect of annealing on cold-rolled Ni – Ti alloys. Mater Sci Eng A. 2008;482:594–7.

13. Helbert G, Saint-Sulpice L, Arbab Chirani S, Dieng L, Lecompte T, Calloch S, et al. Experimental characterisation of three-phase NiTi wires under tension. Mech Mater [Internet]. Elsevier Ltd; 2014;79:85–101. Available from: http://dx.doi.org/10.1016/j.mechmat.2014.07.020

14. Duerig TW, Bhattacharya K. The Influence of the R-Phase on the Superelastic

Behavior of NiTi. Shape Mem Superelasticity [Internet]. Springer International Publishing; 2015;1(2):153–61. Available from: http://link.springer.com/10.1007/s40830-015-0013-4

15. Otsuka K, Wayman CM. Shape Memory Materials. Cambridge. Cambridge University Press; 1998. 284 p.

16. Zhou Y, Zhang J, Fan G, Ding X, Sun J, Ren X, et al. Origin of 2-stage R-phase transformation in low-temperature aged Ni-rich Ti-Ni alloys. Acta Mater. 2005;53(20):5365–77.

17. Jiang F, Liu Y, Yang H, Li L, Zheng Y. Effect of ageing treatment on the deformation behaviour of Ti – 50 . 9 at .% Ni. Acta Mater [Internet]. Acta Materialia Inc.; 2009;57(16):4773–81. Available from: http://dx.doi.org/10.1016/j.actamat.2009.06.059

18. Braga LCM, Silva ACF, Buono VTL, Bahia MG de A. Impact of Heat Treatments on the Fatigue Resistance of Different Rotary Nickel-titanium Instruments. J Endod. 2014;40(9):7–10.

19. Pereira ESJ, Gomes RO, Leroy AMF, Singh R, Peters OA, Bahia MGA, et al. Mechanical behavior of M-Wire and conventional NiTi wire used to manufacture rotary endodontic instruments. Dent Mater. 2013;29:e318–24.

20. Santos LDA, Resende PD, Bahia MGDA, Buono VTL. Effects of R-Phase on Mechanical Responses of a Nickel-Titanium Endodontic Instrument: Structural Characterization and Finite Element Analysis. Sci World J. 2016;2016.

21. Delville R, Malard B, Pilch J, Sittner P, Schryvers D. Transmission electron microscopy investigation of dislocation slip during superelastic cycling of Ni-Ti wires. Int J Plast [Internet]. Elsevier Ltd; 2011;27(2):282–97. Available from: http://dx.doi.org/10.1016/j.ijplas.2010.05.005

22. Heller L, Seiner H, Šittner P, Sedlák P, Tyc O, Kadeřávek L. On the plastic deformation accompanying cyclic martensitic transformation in thermomechanically loaded NiTi. Int J Plast. 2018;(February).

4. FATIGUE RESISTANCE AT DIFFERENT MAXIMUM STRAIN AMPLITUDES OF DUAL-PHASE NiTi WIRES

Jéssica Dornelas Silva*, Pedro Damas Resende, Paula Ribeiro Garcia, Natália Isabel de Azevedo Lopes, Leandro de Arruda Santos, Vicente Tadeu Lopes Buono

Department of Metallurgical and Materials Engineering, Universidade Federal de Minas Gerais (UFMG), Belo Horizonte, MG, Brazil

*Corresponding author: jdornelassilva@gmail.com

Abstract

Known by their functional shape memory and superelastic properties, aligned with an excellent biocompatibility, near equiatomic NiTi alloys are vastly used as biomaterials. In various applications, such as endodontic files and cardiovascular stents, NiTi components are subjected to aggressive fatigue conditions, making fatigue resistance and mechanisms relevant to the material´s development. In this context, heat treatments can be a powerful tool to improve the fatigue life and efforts have been made to understand and predict the fatigue behavior of these alloys in different conditions. In this work, initially superelastic near equiatomic Ni-rich wires were heat-treated at 400°C and 450°C and the ε x Nf curves were obtained. Rotating-bending strain-controlled fatigue tests were performed at maximum strains varying from 1% to 5% at 37°C. The results showed that both samples exhibited large fatigue resistance and similar fatigue behavior through the different maximum strains, and thus, treatments within the range of temperature from 400°C to 450°C are recommended to obtain NiTi components with high fatigue life for large maximum strain amplitudes.

Keywords: nickel-titanium alloys; shape memory; superelasticity; fatigue resistance.

4.1. Introduction

Near equiatomic NiTi alloys are attractive shape memory alloys due to the combination of good mechanical properties with the functional capabilities. Among the wide range of potential applications, NiTi alloys stand out as biomaterials thanks to their high corrosion resistance and biocompatibility, being vastly used on medical and dentistry industries (1,2).

Within these applications, NiTi components are frequently subjected to fluctuating loads and strains, making the fatigue resistance relevant to the material's development. However, the non-linear behavior of these alloys, their complex microstructure, and the influence of the thermomechanical state make fatigue mechanisms hard to understand and their fatigue life difficult to predict (3–5).

Previous works in the literature (6–9) have noted that heat treatments can be effective tools to improve the fatigue resistance of NiTi wires and endodontic files. Figueiredo et al., 2009 (10) and Bahia et al., 2014 (9) have suggested that this improvement is related to the crack branching through the martensite variants resultant from these treatments.

Heat treatments were previously performed on an initially superelastic NiTi wire in a wide range of temperatures from 300°C to 600°C. The heat treated wires that exhibited the best performance in low-cycle fatigue tests with a 4% maximum strain at 37°C were studied in detail in the present wrok. These were the samples heat-treated at 400°C and 450°C and the aim was to obtain the fatigue ε x N curve at 37°C of these samples in order to gain information on fatigue mechanisms in biomedical devices.

4.2. Experimental Procedure

The material used on this study was 1mm diameter 51%Ni-49%Ti heat treated wires in a tubular argon-controlled atmosphere furnace in two different conditions: one heat-treated at 400°C and the other at 450°C for 30 min and then water-quenched. The samples were named S400 and S450, respectively.

X-ray diffraction tests were performed in order to determinate the present phases at room temperature in a PANalytical PW1710 diffractometer. The tests were performed using Cu-Kα radiation and a scan speed of 0.02°/s.

The transformation temperatures were determined by differential scanning calorimetry (DSC) tests, performed at a heating/cooling rate of 10°C/min, ranging from -100°C to 100°C in a Shimadzu DSC-60 calorimeter. The tests were performed in triplicate by cooling each specimen from room temperature to -100°C, following by heating to 100°C, cooling it back to -100°C and heating to room temperature. The reverse transformation temperatures were determined in the interval from -100°C to 100°C, while the direct ones on the subsequent cooling step. Additional DSC tests were

performed by heating the sample from room temperature (22°C) up until 50°C aiming to evaluate how the samples behave when heated up until the fatigue test temperature.

Tensile tests were carried out in a heating chamber at 37°C in an Instron 5582 testing machine in order to evaluate the mechanical behavior of the wires. In accordance to ASTM F2516−14 standard (11), tests until rupture were performed at a crosshead speed of 12 mm/min and loading and unloading up to 6% deformation at a crosshead speed of 1.2 mm/min. The experiments were repeated three times.

Finally, the fatigue tests took place in a proper flexural fatigue machine at 1%, 2%, 3%, 4% and 5% maximum strains in controlled temperature at 37°C (7). Each experiment was performed with 5 different specimens and a t-test was made.

4.3. Results

The diffractograms obtained for S400 and S450, Fig. 1, showed that these samples were constituted mainly by the R-phase at room temperature, as indicated by the splitting of the $(100)_{B2}$ peak into the $(11\text{-}2)_R$ and $(300)_R$ peaks (12,13).

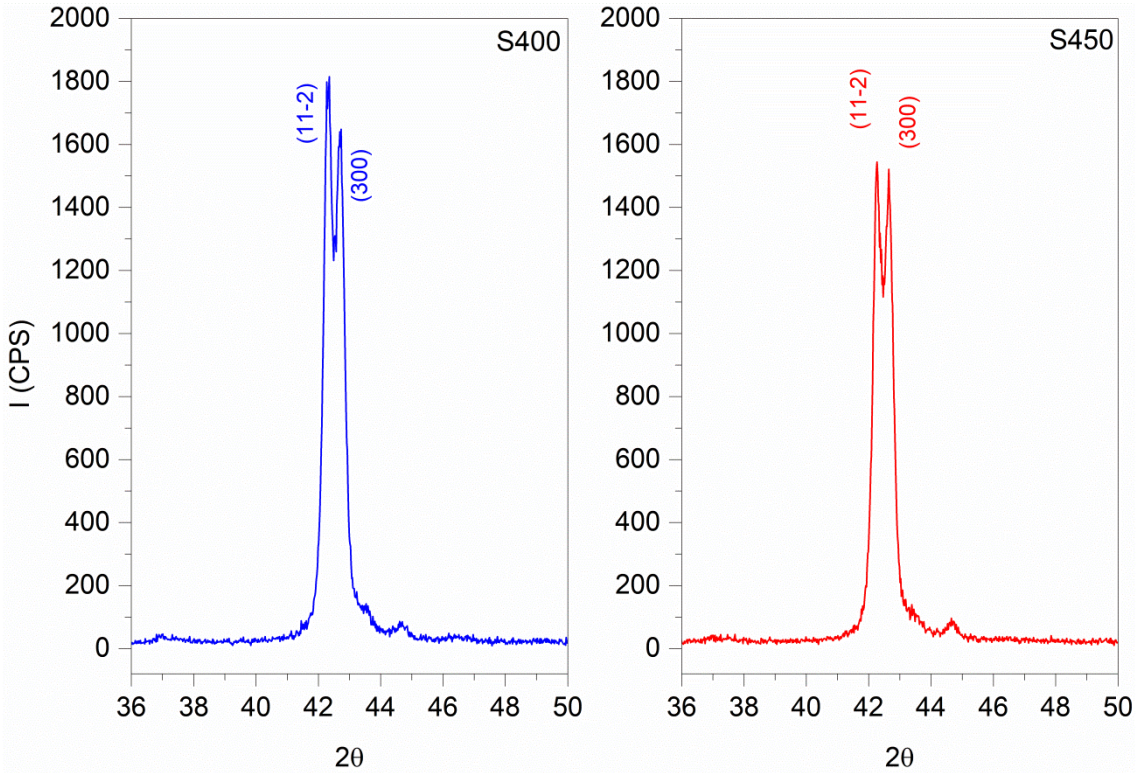

Figure 4.1 – R-phase peaks on the XRD results of S400 and S450.

The DSC charts are shown in Figure 2 and both samples presented similar transformation behavior. Near equiatomic Ni-rich alloys undergo martensitic

transformations involving the high temperature austenitic B2 phase and the low-temperature martensitic B19' phase. Additionally, when coherent Ti_3Ni_4 precipitates are present, the martensitic transformation can occur in two steps, involving the formation of the pre-martensitic R-phase (14).

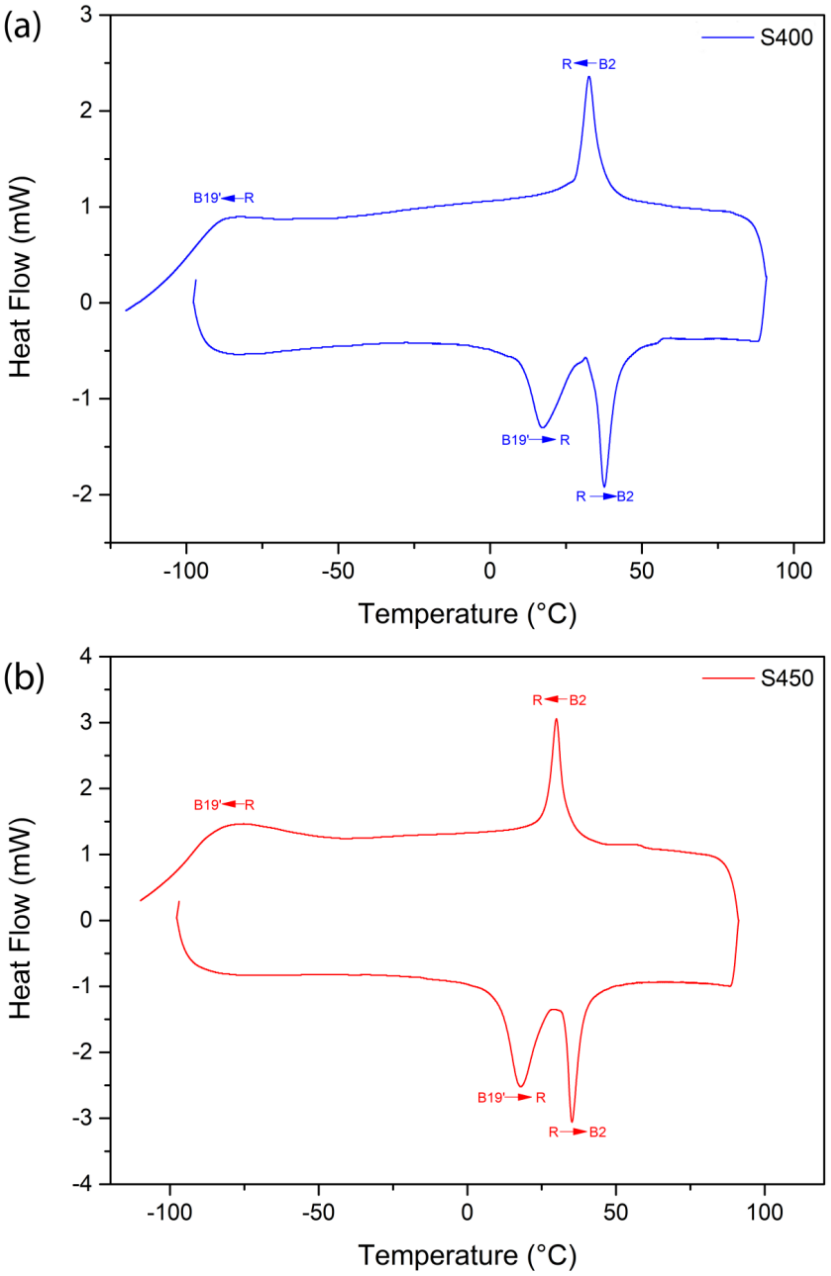

Figure 4.2 – Representative DSC charts for (a)S400 and (b)S450**.**

During heating, two-peak transformations were detected, while on cooling a well-defined sharp peak appeared in the two samples, followed by a flat low-temperature peak. The sharp peaks, with a small temperature hysteresis between heating and cooling, are typical from the B2 ↔ R transformation (WANG et al., 2014), in

agreement with the XRD results. The broader peaks are related to B19' ↔ R-phase transformations (15,16)

When the samples were heated from room temperature, only one heating peak could be observed, as it can be seen in Figure 3. In this case, the samples heat up from an R-phase structure and the detected peak refers to the R → B2 transformation. Thus, at 37°C, the temperature at which the fatigue tests were performed, both samples were constituted by austenite + R-phase microstructures. Sample S450, due to its lower reverse transformation temperatures should have more austenite than S400.

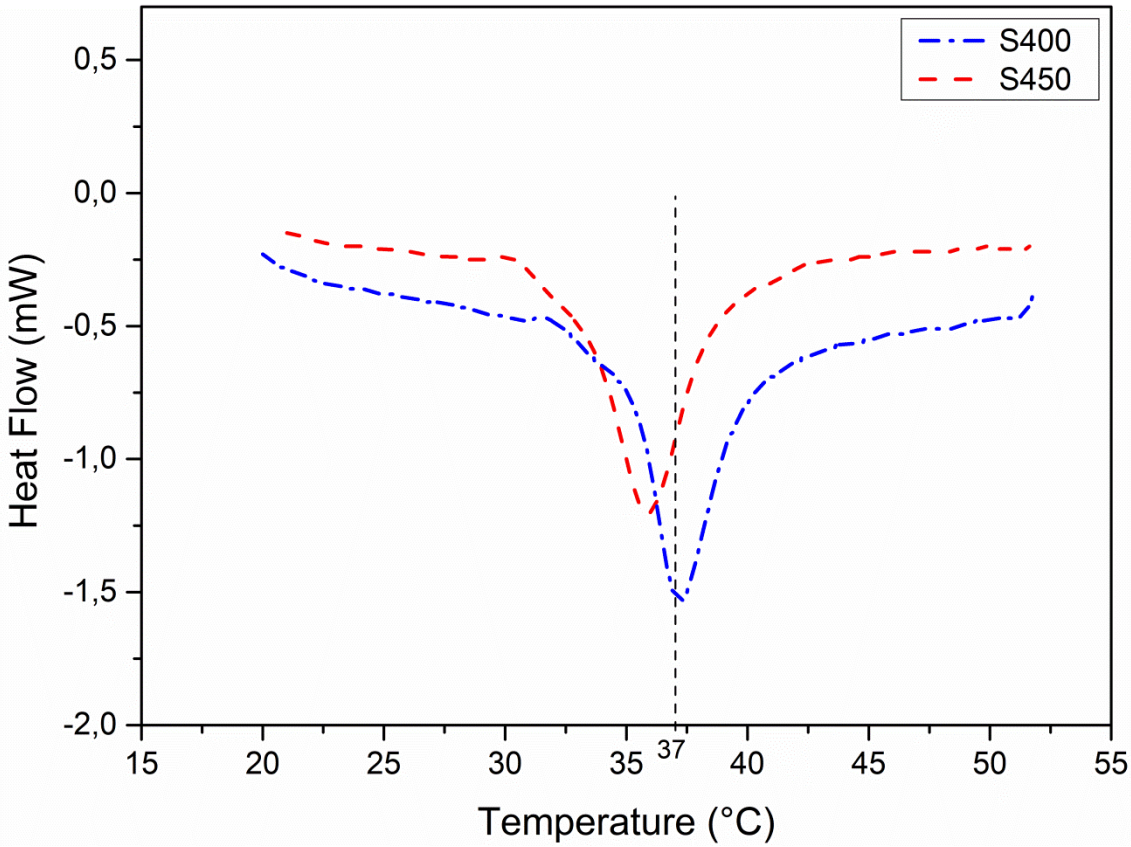

Figure 4.3 – Representative DSC charts during heating from room temperature**.**

When tested in tension, both samples presented similar behavior until rupture, as shown in Figure 4. S400 presented a slightly higher ultimate tensile strength. The insert in the figure shows the behavior of samples deformed to 6% total strain and then unloaded to zero load. It can be seen that both samples exhibited partial superelastic behavior. When the samples were heated, the remaining deformation could be recovered, constituting the shape memory effect.

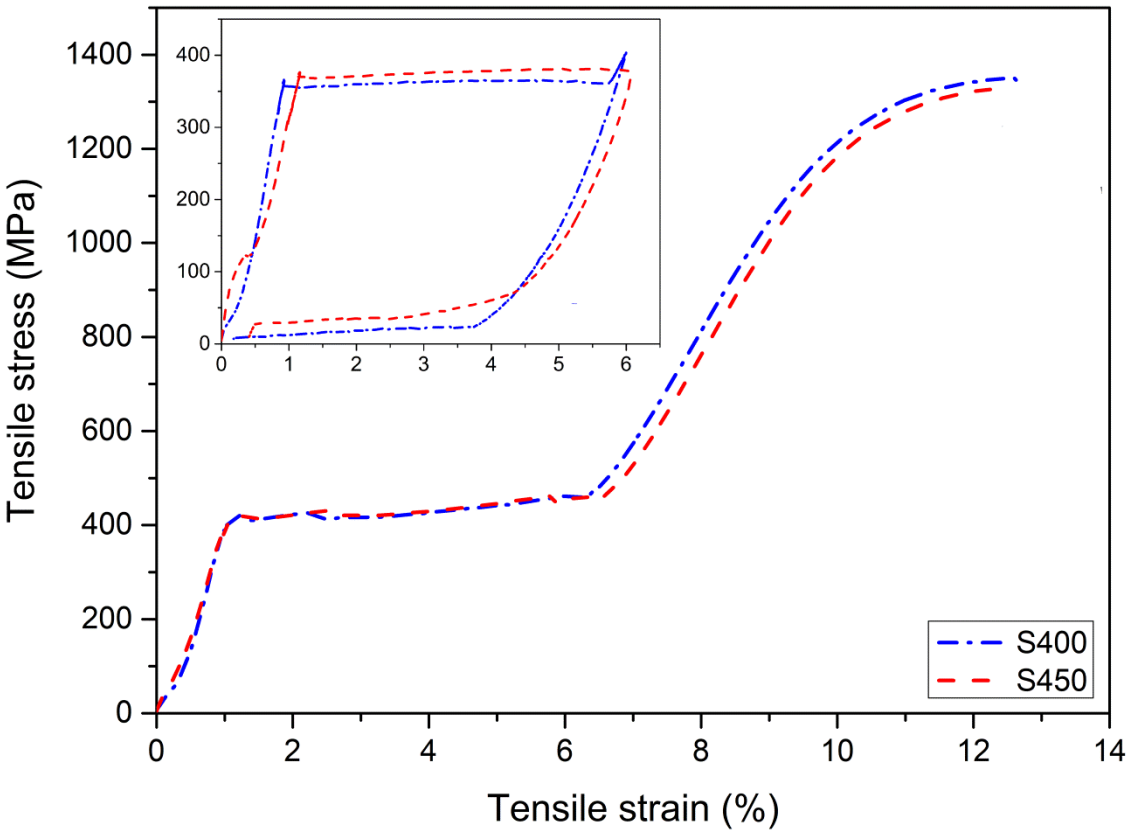

Figure 4.4 – Representative stress vs strain curves at 37°C for S400 and S450**.**

The ε x Nf curves are plotted in Figure 5 and the p-values are shown above each condition. It is possible to observe that there is a tendency in increasing the number of cycles to failure in S450 from 5% on. The behavior of S400 within the range 5% to 3% is more difficult to describe because of the dispersion of the results, although the increase in the number of cycles to failure was similar for both samples after 3% strain. The samples tested with the smallest strain employed, 1%, failed in a number of cycles higher than 30,000 and are not presented in the graph. Samples that presented p-values lower than 0.05 are considerate statiscally different and samples that presented p-values higher than 0.05 are considerate statiscally the same.

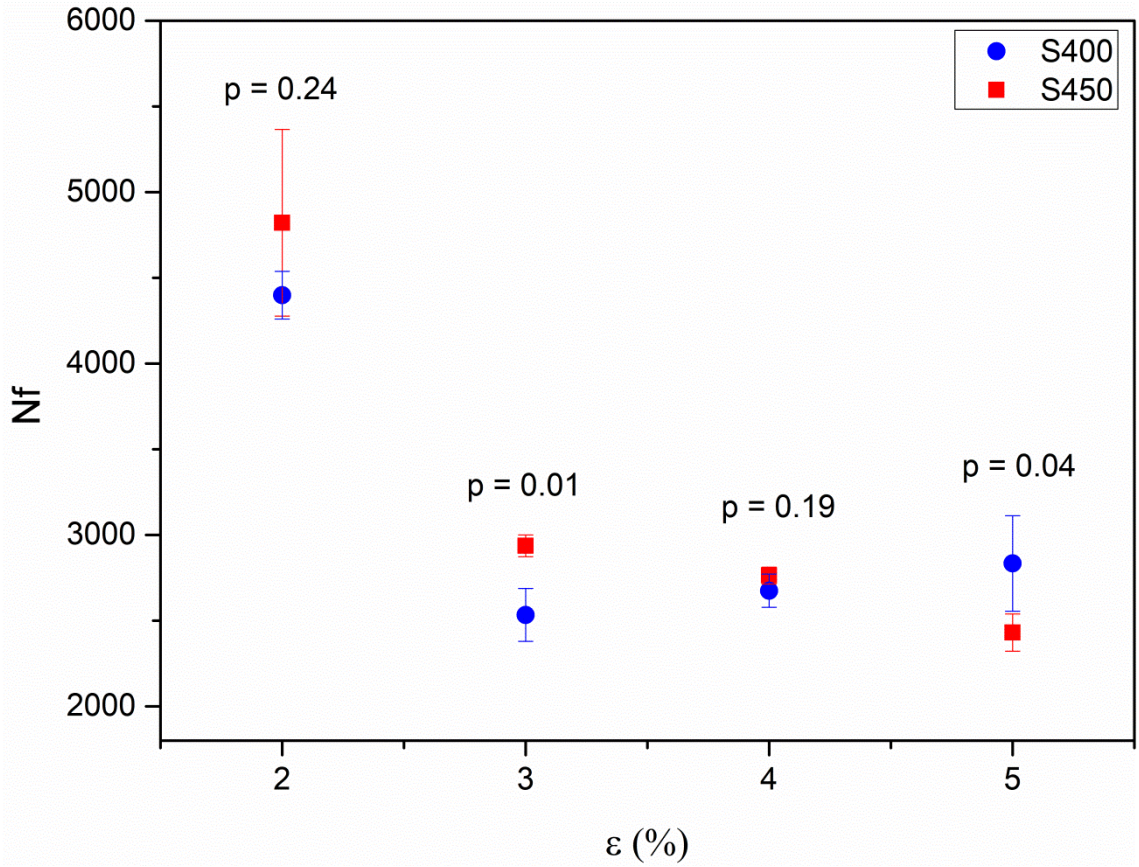

Figure 4.5 – Maximum applied strain ε vs number of cycle to failure Nf obtained in the rotating-bending fatigue tests at 37°C for S400 and S450.

4.4. Discussion

The heat treatments performed in this study produced structures with similar mechanical and transformation behaviors. At 37°C, both of them presented dual phase structures constituted by austenite and R-phase with different phase fractions. From the DSC charts, it is possible to assume that the fraction of austenite formed by heating up until the test temperature is higher in S450 than in S400, since the second sample presented a higher transformation peak temperature.

The increase in the peak transformation temperature from S400 to S450 also indicates that a higher fraction of precipitates is present at S450, depleting the matrix from soluble Ni. On the other hand, the higher ultimate tensile strength of S400 indicates that its precipitates are small and finely dispersed in the matrix. In that case, it is possible to infer that S450 presents larger precipitates than S400.

The results of the fatigue tests are consistent with the conclusion that wires with higher amounts of R-phase are less sensitive to the maximum applied strain in aggressive strain

conditions. Nevertheless, a high number of cycles to failure could be achieved at the most aggressive tested condition, 5% strain. On the other hand, the wires which apparently contain a higher fraction of austenite, S450, exhibited a slightly lower fatigue resistance when the maximum strain was increased within this range. It is also worth noting that S450 presented higher fatigue predictability in these strains, as also observed by Arias et al., 2018 (17) in endodontic files tested in low-cycle fatigue.

It is also worth noting that, when comparing the obtained number of cycles at these strains for S400 and S450 with superelastic wires and endodontic files reported in the literature (3,10,18,19), the fatigue resistance of S400 and S450 is considerably high at 3% to 5% maximum strains.

A change on the fatigue regime can be observed from 3% to 2% maximum strains, where the slope of the curves change and the number of cycles to failure increases significantly. Between 2% and 1%, S400 and S450 presented approximately the same fatigue resistance considering the dispersion. A change on the fatigue mechanisms can be inferred by the large dispersion for S450 at 2% maximum strain, which cannot be observed in more aggressive conditions.

Finally, when comparing the number of cycles to failure from one sample to the other, despite of the 50°C difference on the heat-treating temperature and potential differences in the austenite/R-phase relative fraction, only small statistical differences were observed on the fatigue life of the heat treated wires for 5% and lower maximum strains. Hence, when producing near equiatomic Ni-rich NiTi biomaterials, heat-treating at temperatures within this range will result in structures with a good fatigue performance.

4.5. Conclusions

In this paper, the strain controlled ε x Nf fatigue curve at 37°C was obtained for Ni-rich near equiatomic wires heat-treated at 400°C (S400) and 450°C (S450). At room temperature, both S400 and S450 presented R-phase structures. At body temperature, both of them were constituted by austenite + R-phase, exhibiting a high amount of superelasticity. S450 likely presented a higher amount of austenite than S400.

Overall, it can be noted that S400 and S450 presented similar mechanical response under static and cyclic bending-rotating loading and higher amounts of the R-phase seem to be beneficial when increasing the maximum strain in the low-cycle regime. The

results obtained in this study indicate that heat treatments within the range from 400°C to 450°C are recommended to obtain a good fatigue life at body temperature, especially in aggressive straining conditions.

Acknowledgements

This work was supported by Conselho Nacional de Desenvolvimento Científico e Tecnológico (CNPq), Coordenação de Aperfeiçoamento de Pessoal de Nível Superior (CAPES/PROEX) and the Fundação de Amparo à Pesquisa de Minas Gerais (FAPEMIG).

References

1. Otsuka K, Wayman CM. Shape Memory Materials. Cambridge. Cambridge University Press; 1998. 284 p.

2. Feninat F El, Laroche G, Fiset M, Mantovani D. Shape Memory Materials for Biomedical Applications. Adv Eng Mater. 2002;4(3):91–104.

3. Runciman A, Xu D, Pelton AR, Ritchie RO. An equivalent strain/Coffin-Manson approach to multiaxial fatigue and life prediction in superelastic Nitinol medical devices. Biomaterials [Internet]. Elsevier Ltd; 2011;32(22):4987–93. Available from: http://dx.doi.org/10.1016/j.biomaterials.2011.03.057

4. Kollerov M, Lukina E, Gusev D, Mason P, Wagstaff P. Impact of material structure on the fatigue behaviour of NiTi leading to a modified Coffin-Manson equation. Mater Sci Eng A [Internet]. Elsevier; 2013;585:356–62. Available from: http://dx.doi.org/10.1016/j.msea.2013.07.072

5. Allegretti D, Francesca Berti B, Francesco Migliavacca B, Giancarlo Pennati B, Petrini L. Fatigue Assessment of Nickel–Titanium Peripheral Stents: Comparison of Multi-Axial Fatigue Models. Shape Mem Superelasticity [Internet]. Springer International Publishing; 2018;4(1):186–96. Available from: https://doi.org/10.1007/s40830-018-0150-7

6. Bahia MG de A, Dias RF, Buono VT. The influence of high amplitude cyclic straining on the behaviour of superelastic NiTi. Int J Fatigue. 2006;28(9):1087–91.

7. Pereira ESJ, Gomes RO, Leroy AMF, Singh R, Peters OA, Bahia MGA, et al. Mechanical behavior of M-Wire and conventional NiTi wire used to manufacture rotary endodontic instruments. Dent Mater. 2013;29:e318–24.

8. Shen Y, Zhou H, Zheng Y, Peng B, Haapasalo M. Current Challenges and Concepts of the Thermomechanical Treatment of Nickel-Titanium Instruments. J Endod [Internet]. Elsevier Ltd; 2013;39(2):163–72. Available from: http://dx.doi.org/10.1016/j.joen.2012.11.005

9. Braga LCM, Silva ACF, Buono VTL, Bahia MG de A. Impact of Heat Treatments on the Fatigue Resistance of Different Rotary Nickel-titanium Instruments. J Endod. 2014;40(9):7–10.

10. Figueiredo AM, Modenesi P, Buono V. Low-cycle fatigue life of superelastic NiTi wires. Int J Fatigue [Internet]. Elsevier Ltd; 2009;31(4):751–8. Available from: http://dx.doi.org/10.1016/j.ijfatigue.2008.03.014

11. Standard test method for tension testing of nickel-titanium superelastic materials. ASTM - F2516. 2015. p. 1–6.

12. Wang XB, Verlinden B, Van Humbeeck J. R-phase transformation in NiTi alloys. Mater Sci Technol [Internet]. 2014;30(13):1517–29. Available from: http://www.tandfonline.com/doi/full/10.1179/1743284714Y.0000000590

13. Santos LDA, Resende PD, Bahia MGDA, Buono VTL. Effects of R-Phase on Mechanical Responses of a Nickel-Titanium Endodontic Instrument: Structural Characterization and Finite Element Analysis. Sci World J. 2016;2016.

14. Otsuka K, Ren X. Physical metallurgy of Ti – Ni-based shape memory alloys. Prog Mater Sci. 2005;50:511–678.

15. Helbert G, Saint-Sulpice L, Arbab Chirani S, Dieng L, Lecompte T, Calloch S, et al. Experimental characterisation of three-phase NiTi wires under tension. Mech Mater [Internet]. Elsevier Ltd; 2014;79:85–101. Available from: http://dx.doi.org/10.1016/j.mechmat.2014.07.020

16. Duerig TW, Bhattacharya K. The Influence of the R-Phase on the Superelastic Behavior of NiTi. Shape Mem Superelasticity [Internet]. Springer International

Publishing; 2015;1(2):153–61. Available from: http://link.springer.com/10.1007/s40830-015-0013-4

17. Arias A, Macorra JC, Govindjee S, Peters OA. Correlation between Temperature-dependent Fatigue Resistance and Differential Scanning Calorimetry Analysis for 2 Contemporary Rotary Instruments. J Endod. 2018;44(4):630–4.

18. Robertson SW, Pelton AR, Ritchie RO. Mechanical fatigue and fracture of Nitinol. Int Mater Rev [Internet]. 2012;57(1):1–37. Available from: http://www.tandfonline.com/doi/full/10.1179/1743280411Y.0000000009

19. Tyc O, Pilch J, Sittner P. Fatigue of superelastic NiTi wires with different plateau strain. Procedia Struct Integr [Internet]. Elsevier B.V.; 2016;2:1489–96. Available from: http://linkinghub.elsevier.com/retrieve/pii/S2452321616301998

5. THE EFFECT OF LOW-TEMPERATURE HEAT-TREATMENT ON THE TENSILE AND FATIGUE BEHAVIOR OF AN INITIALLY SUPERELASTIC NITI WIRE

Jéssica Dornelas Silva*, Pedro Damas Resende, Natália Isabel de Azevedo Lopes, Leandro de Arruda Santos, Vicente Tadeu Lopes Buono

Department of Metallurgical and Materials Engineering, Universidade Federal de Minas Gerais (UFMG), Belo Horizonte, MG, Brazil

*Corresponding author: jdornelassilva@gmail.com

Abstract

Aging treatments are powerful tools for controlling the martensitic transformation temperatures of near-equiatomic Ni-rich NiTi. Due to the precipitation of Ni-rich particles, changes may be observed in the transformation temperatures, but they also affect the mechanical behavior of the material in ways that are not yet clearly understood. In this context, this study aims to evaluate the effect of a 400°C heat treatment on the tensile and fatigue properties of an initially superelastic near-equiatomic Ni-rich NiTi wire. For that, tensile tests were performed until rupture and loading/unloading tests were performed until 6% deformation in both as-received and heat treated conditions. Additionally, rotating-bending strain-controlled fatigue tests were performed at 4% maximum strain in controlled temperatures at 25°C and 37°C. The results obtained showed that the heat treatment promoted the formation of the R-phase, increased the fatigue resistance significantly, hardened the structure and facilitated the formation of stress-induced martensite. The increase on the test temperature resulted in decrease in the fatigue life.

Keywords: nickel-titanium alloys; shape memory; superelasticity; heat-treatment, fatigue resistance.

5.1. Introduction

Near-equiatomic NiTi alloys are known to be the most commercially used shape memory alloys. These alloys undergo a thermoelastic martensitic transformation from a high temperature austenitic B2 structure to a low-temperature martensitic B19' structure, exhibiting both shape memory effect and superelasticity. Their functional properties

combined with good corrosion resistance make them suitable to a wide range of applications in couplings, actuators, sensors, biomedical and dental appliances (1–4).

Thermal and thermomechanical treatments are successfully used to control transformation temperatures of Ni-rich near equiatomic NiTi shape memory alloys. These treatments promote precipitation reactions that are followed by increases in the martensitic transformation start temperature due to the decrease in the Ni content of the matrix. Besides that, the strain fields generated by coherent Ti_3Ni_4 particles favors the appearance of a rhombohedral pre-martensitic phase, the R-phase, and the occurrence of a two-step phase transformation (5–8).

Changes in the transformation temperatures and thermomechanical state promoted by heat-treating NiTi alloys are accompanied by changes on both functional and mechanical properties (9–11). However, the complex behavior of these alloys is not yet clearly understood (12,13). In this context, the aim of this study is to evaluate the effect of a heat treatment at 400°C for 30 min on the mechanical behavior of an initially superelastic NiTi wire and the effect of the test temperature on the fatigue life of similar initial microstructures.

5.2. Experimental Procedure

Commercial austenitic superelastic NiTi wires with 1 mm in diameter, previously annealed and pickled, with a nominal composition of 51 at. %Ni - 49%Ti, were used in this study. 12 cm long specimens of the as-received wire (AR) were heat treated in a tubular furnace at 400°C for 30 minutes in an argon atmosphere and then quenched in water at room temperature. The heat treated samples were named HT.

X-ray diffraction (XRD) analyses were performed with 2θ ranging from 30° to 120° for phase identification at room temperature using Cu-Kα (λ = 0.15418 nm) radiation and a scan speed of 0.02°/s. The peaks were identified by comparison with patterns from the ICSD database and spectra available in the literature (14–17).

The martensitic direct (Ms, Mf) and reverse (As, Af) transformation temperatures were determined by differential scanning calorimetry (DSC) at a cooling/heating rate of 10°C/min. The tests were performed in triplicate by cooling each specimen from room temperature to -100°C, following by heating to 100°C, cooling it back to -100°C and heating to room temperature. The reverse transformation temperatures were determined

in the heating interval from -100°C to 100°C, while the direct ones on the subsequent cooling step.

Tensile tests were carried out according to ASTM F2516 (18). Tests until rupture were performed at a crosshead speed of 12 mm/min. Other specimens were loaded up to 6% deformation and then unloaded to zero stress, at a crosshead speed of 1.2 mm/min. The experiments were repeated three times.

Fatigue tests were performed in the bending-rotating apparatus shown in Figure 1. The maximum strain amplitude was 4% and the tests were conducted in water baths at 25°C and 37°C. The fracture surfaces were analyzed by scanning electron microscopy (SEM).

Figure 5.1 – Bending-rotating fatigue test apparatus.

5.3. Results

Figure 2 shows the XRD spectra obtained for the as received (AR) and the heat treated (HT) samples. It can be observed (Figure 2-a) that the AR sample exhibited, as expected, an austenitic pattern characterized by a high intensity (110) peak at 2θ = 42.5°. On the other hand, the HT sample (Figure 2-b) has shown an essentially R-phase spectrum, similar to the one observed by other authors (14,19). It has been noted that the diffraction pattern of the R-phase, comparing to that of the austenitic phase, exhibits the splitting of the (110) B2 and (211) B2 peaks, like observed in Figure 2, while the (002) B2 peak remains unchanged (16).

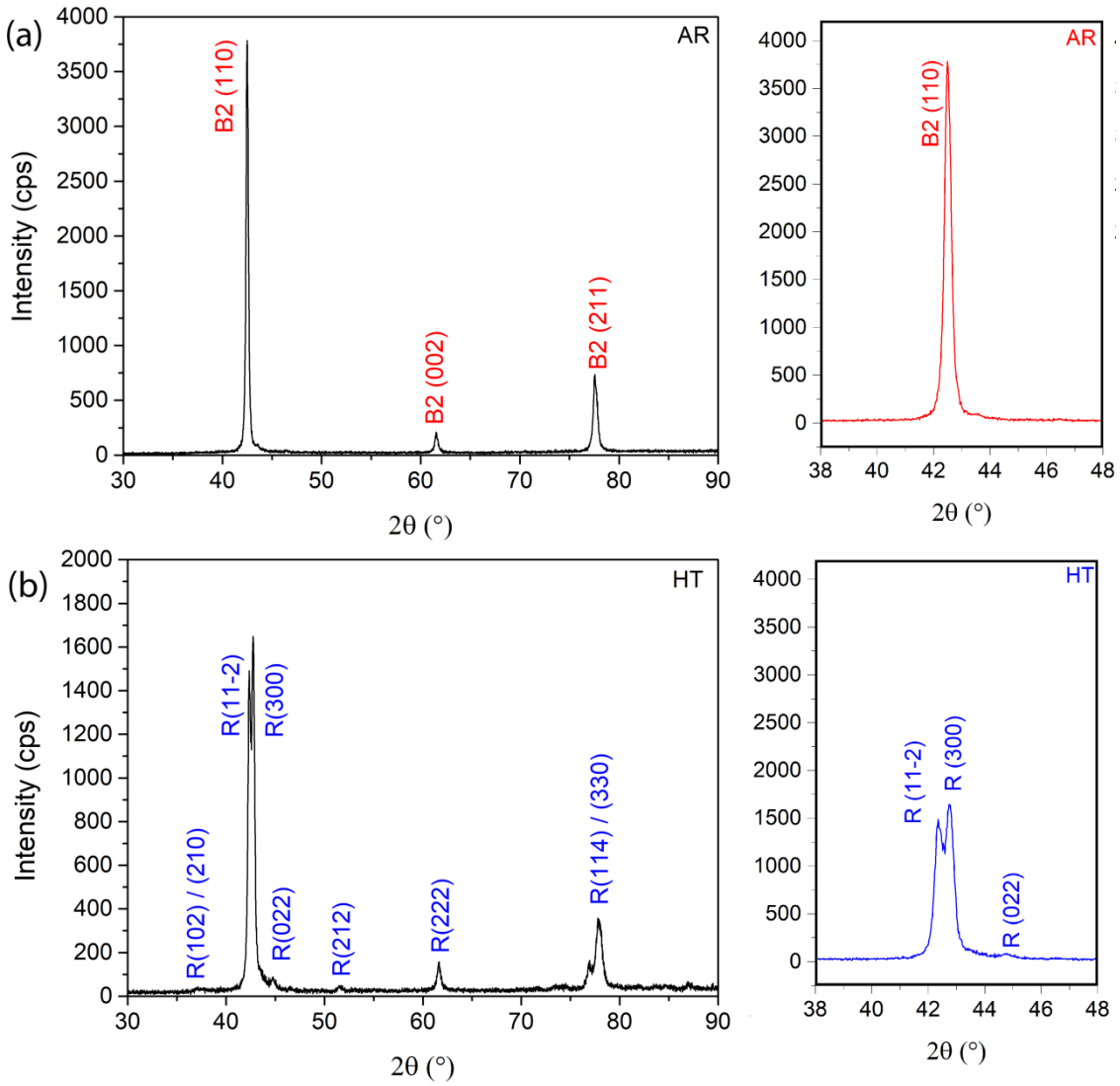

Figure 5.2 - XRD spectra obtained for (a) as received sample and (b) heat treated sample**.**

The DSC charts are presented in Figure 3. The AR chart has shown peaks of direct transformations during cooling (B2 → B19') and during heating (B19' → B2). In contrast, the 400°C chart presented a sharp peak during cooling and well defined two peaks during heating. In agreement to the XRD results, the sharp profile of the cooling peak and the second heating peak, and the small hysteresis between these two peaks are characteristic of R-phase transformation peaks. Thereby, during cooling, the peak observed refers to a B2 → R transformation, leading to the R-phase structure at room temperature. The R → B19' transformation could not be observed, but the corresponding peak is reported (20,8) to be difficult to detect due to its flatness and/or to an incomplete transformation at the lower temperature limit of the test. During

heating, the first and broader peak is related to the B19' → R-phase transformation, confirming the occurrence of a martensite transformation during cooling, even though the R → B19' transformation peak could not be detected. The second and sharper peak upon heating refers to the R-phase → B2 transformation, characterizing a symmetric R-phase transformation, as suggested by Duerig et al, 2015 (8).

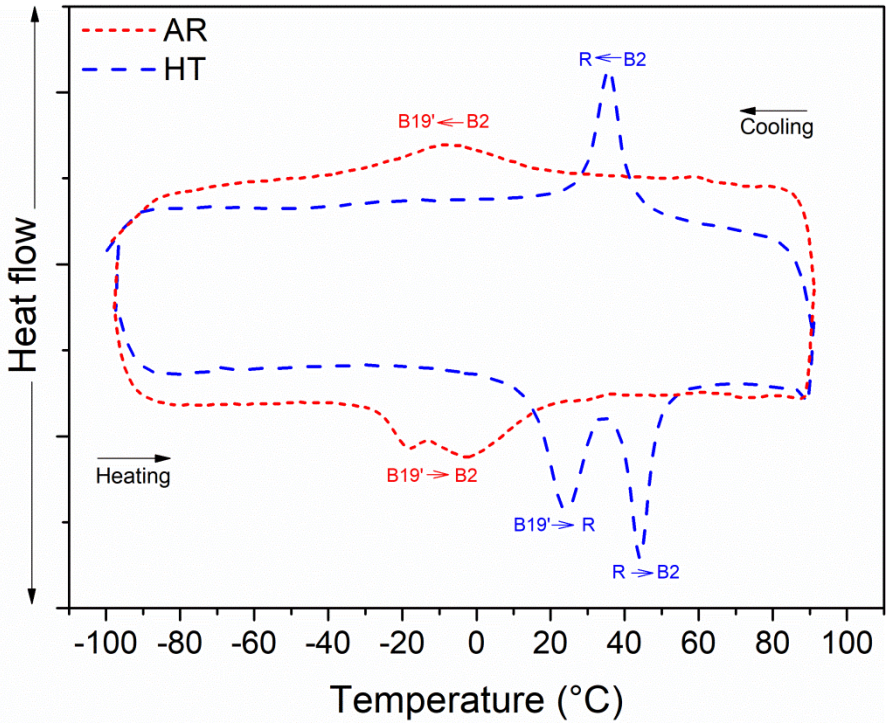

Figure 5.3 - Representative DSC charts for as received and heat treated samples**.**

To check this hypothesis, an additional DSC analysis was made in HT starting at 90°C, cooling to 0°C, and then heating again to 90°C at the same cooling/heating rate of 10°C/min. The DSC chart obtained is presented in Figure 4. It can be observed that the transformation during heating was no longer in two-steps. This fact confirms that, in this study, the first peak in Fig. 3 was related to an undetected R → B19' transformation at low-temperatures, rather than to the occurrence of heterogeneous precipitation like previously observed by Khallil-Allafi et al. (5,6,21).

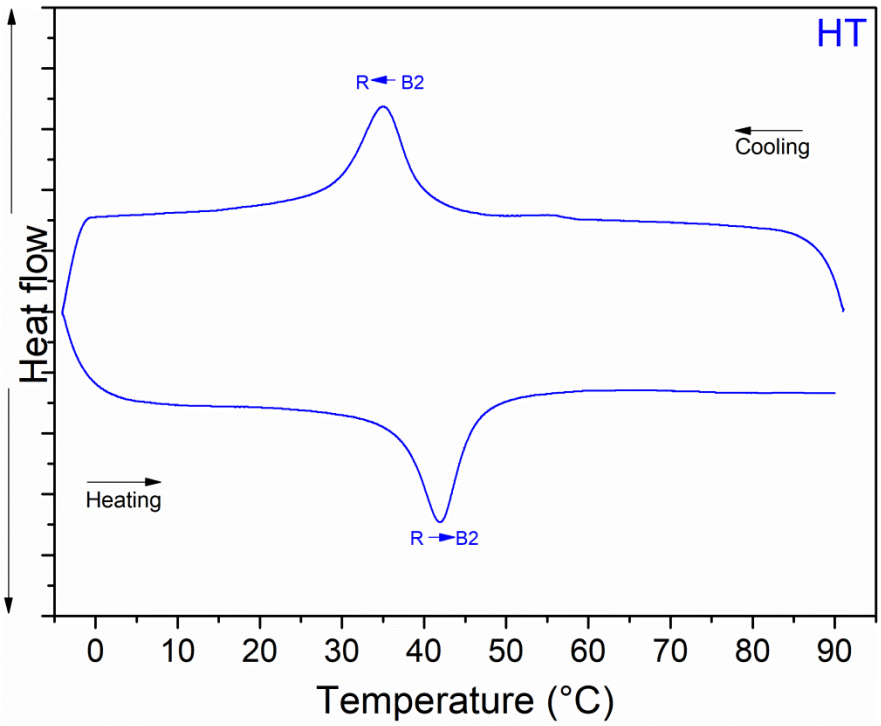

Figure 5.4 – DSC chart for the heat treat sample from 0°C to 90°C.

The mean transformation temperatures from the DSC analysis are presented in Table 1, where Ts and Tf refer, respectively, to Ms and Mf in AR and to Rs and Rf in HT. A significant increase of 30°C in the austenitic finishing temperature Af can be observed in the heat-treated sample.

Table 5.1 – Transformation temperatures as a function of sample condition

	As (°C)	**Af (°C)**	**Ts (°C)**	**Tf (°C)**
AR	-29	19	19	-38
HT	16	49	43	32

The obtained tensile stress vs strain curves are presented in Figure 5. In the rupture curves (Figure 5-a), it can be seen that the heat treatment resulted in a decrease of the stress plateau, an increase in the strain obtained during the stress plateau and in an increase in the ultimate tensile stress. In the loading/unloading tests, AR presented superelastic behavior while a large amount of residual strain was observed in HT. A full shape recovery of the deformed HT could be achieved by heating it to a temperature above the measured Af, characterizing the shape memory effect.

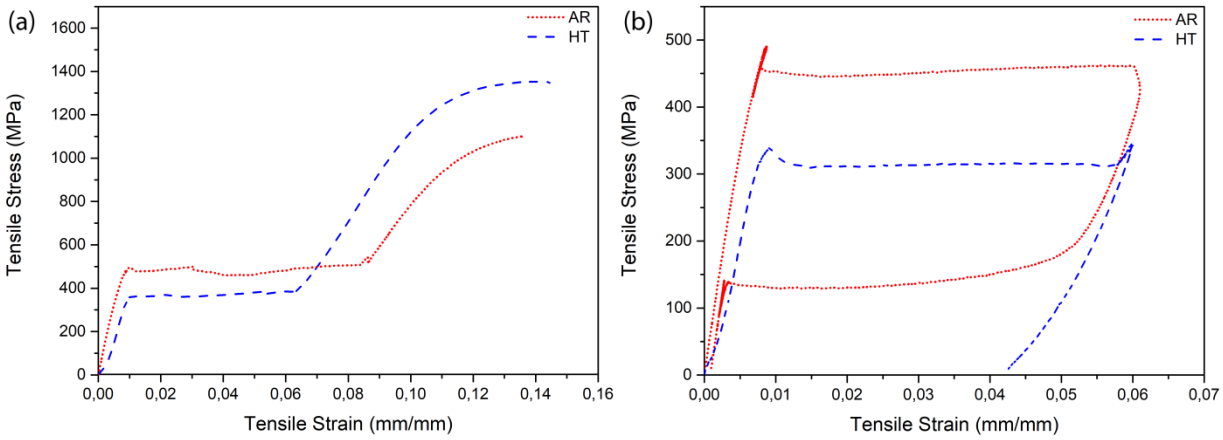

Figure 5.5 – Representative stress x strain curves obtained from tensile testing (a) until rupture and (b) loading/unloading**.**

From the tensile curves, it was possible to estimate the austenite and R-phase apparent elastic moduli (E_a) in the analyzed conditions as well as the stress required for the induction of martensite (σ_{MI}) from austenite (AR) and R-phase (400°C), considering the load-unload tests, while the tensile strength (σ_u) was determined from the rupture tests. Mean values of these properties are presented in Table 2.

Table 5.2 – Mean values of elastic moduli, martensitic induced transformation stress and tensile strength obtained from tensile tests

	E (GPa)	**σ_{MI} (MPa)**	**σ_u (MPa)**
AR	65.6	443.9	1092.9
HT	48.2	330.0	1304.7

Finally, Figure 6 presents the mean number of cycles to failure in each condition while the characteristic features of the fracture surfaces are shown in Figure 7. It is possible to observe that the heat treatment improved the fatigue resistance of the AR wire at both test temperatures, 25°C and 37°C. When comparing samples tested at 25°C and samples tested at 37°C, it is possible to see a tendency to decrease the number of cycles to failure with increasing temperature.

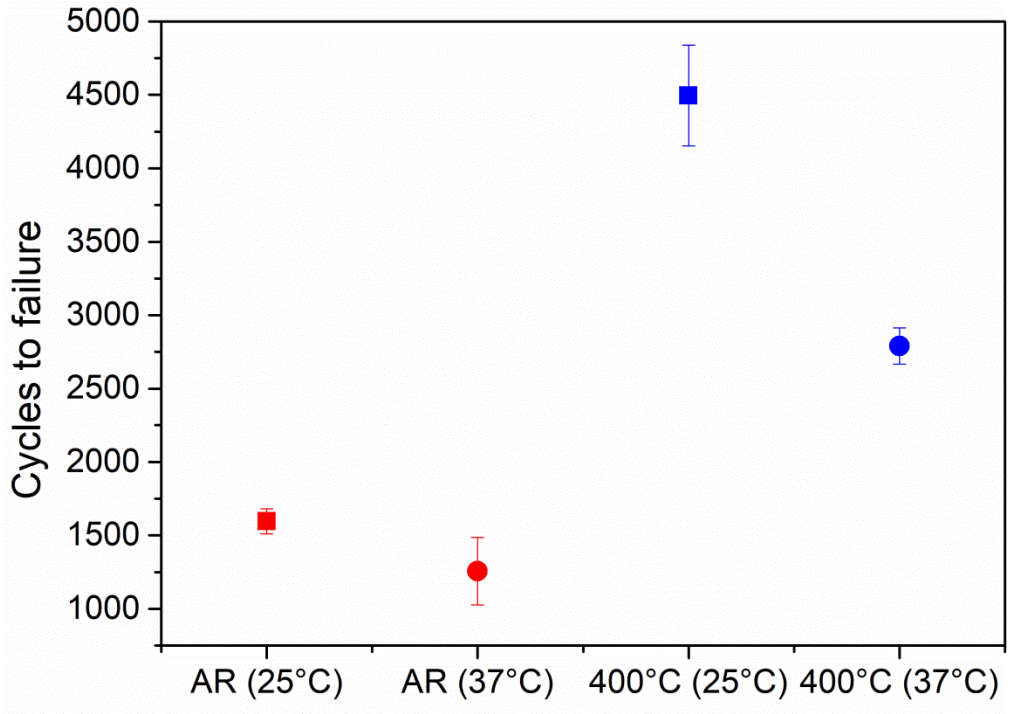

Figure 5.6 – Mean number of cycles to failure obtained for the as received and the heat treated samples at 25°C and 37°C.

The fracture surface of the fatigue tested samples presented two different regions: a slow crack propagation region and a ductile final propagation region, and a transition zone between them. The slow crack propagation region is characterized by the presence of fatigue striations, as it can be seeing in Figure 7 (b, e, h and k), and the ductile fracture region, by the presence of microvoids or dimples, in evidence in Figure 7 (c, f, i and l). The transition zone is constituted by a mixture of striations and dimples. The slow crack propagation is delimited and smaller sites of fatigue propagation observed along the surface are indicated by arrows in Fig. 7 (a, d, g, and j).

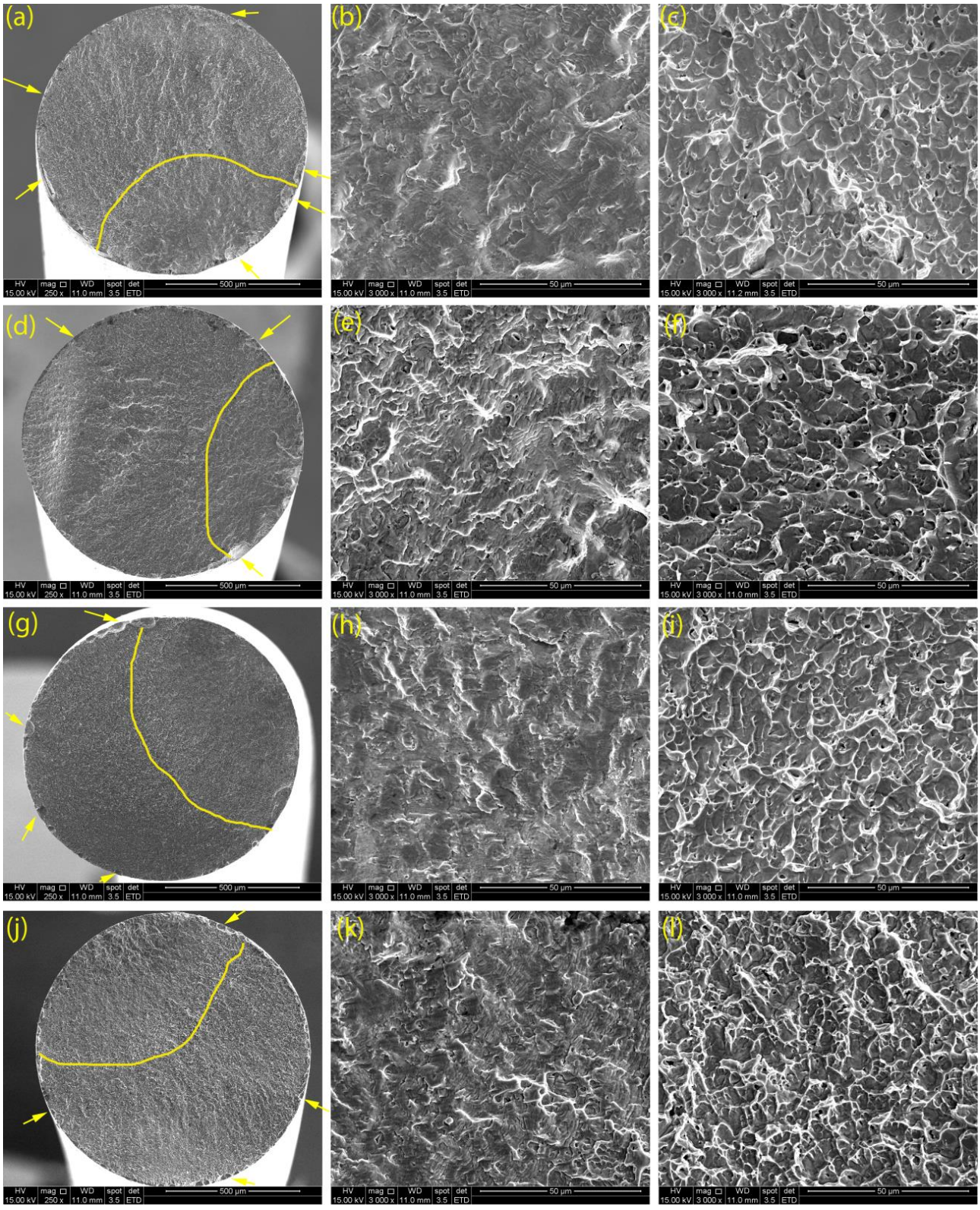

Figure 5.7 – Fatigue crack surfaces for (a), (b) and (c) AR tested at 25°C; (d), (e) and (f) AR tested at 37°C;(g), (h) and (i) HT tested at 25°C and (j), (k), (l) HT tested at 37°C.

5.4. Discussion

According to the results obtained in this study, the AR wire presents austenitic structure and superelastic behavior at room temperature, as expected. The flat cooling DSC peak and the “break” on the heating peak can be indications of a state of high strain hardening and high microstructure heterogeneity resulting from the wire fabrication processes. The heat treatment at 400°C for 30 min resulted in a fatigue resistant R-phase structure at room temperature that presented shape memory effect. The presence of the R-phase and the increases in the transformation temperatures and in the tensile strength indicate that the precipitation of coherent Ti_3Ni_4 particles occurred during the performed heat treatment.

In the tensile tests, the AR samples undergo elastic deformation in the austenitic structure until a critical stress is reached and a stress plateau is observed. The stress plateau, in which strains of around 8% could be achieved, is related to the formation of stress-induced martensite. When loaded up to 6% and then unloaded, the strain was almost completely recovered by means of the reverse transformation.

In the heat-treated samples, the plateau also represents the formation of B19’martensite induced by stress but starting from the R-phase. In this case, the initially thermally-induced R-phase variants undergo detwinning in the initial stages of loading. This phenomenon takes place at very low stresses (16,22) and is observed as an initial instability on the stress-strain curve. The oriented R-phase deforms elastically until the plateau stress is reached and martensite is induced by tension. This phase transformation requires a lower stress level than in B2 -> B19' since the barrier to transforming martensite from R-phase is smaller than from austenite. The lattice strain produced during this transformation is smaller than the previous, indicated by the plateau length.

During unloading, a small shape recovery is observed, attributed both to the elastic recovery and to a partial B19’->R transformation like suggested by Duerig et al. (8). From the DSC chart, it is possible to point out that room temperature (25°C) is in a region below Rf and above As where both the R-phase and a hybrid martensitic/R-phase structure are stable, depending on whether it is resulted from cooling or heating. While deforming the sample, disturbances on the system can be responsible for the occurrence of some B19’ -> R phase reverse transformation, resulting in a two-phase martensite/R-

phase oriented structure. This hypothesis is endorsed by an XRD analysis performed in a tensile tested sample (Figure 8), which presented R-phase and martensitic peaks.

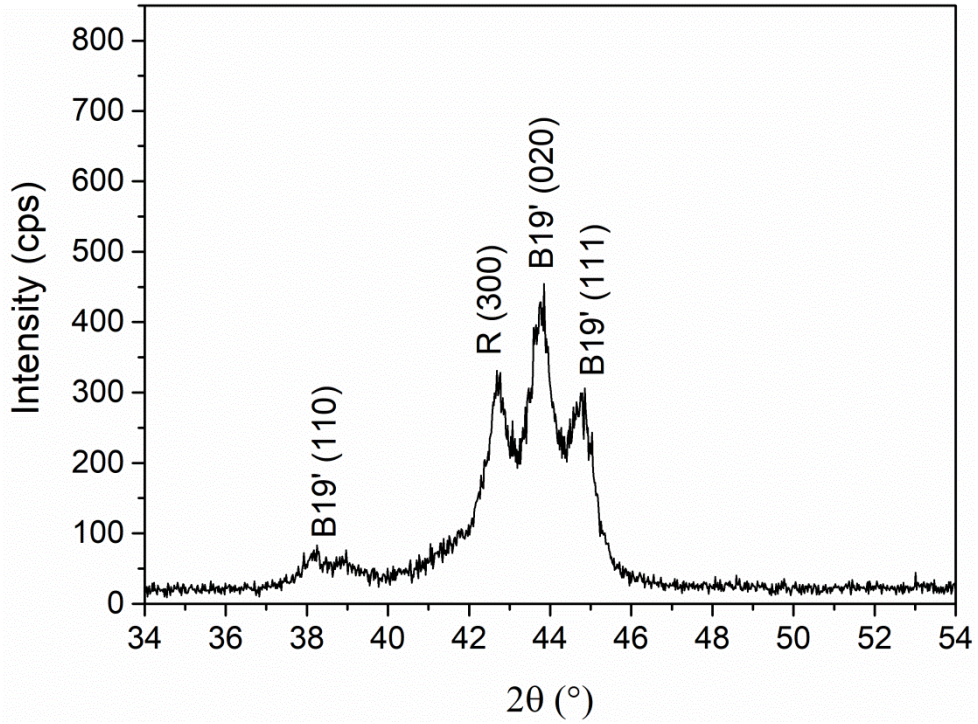

Figure 5.8 – XRD spectra obtained for a heat treated sample tested in the loading/unloading tensile test**.**

Finally, the fatigue tests have shown a significant increase in fatigue resistance of the heat-treated samples. By relating the test temperatures to the XRD and DSC results, it is possible to assume that the AR samples exhibited an austenitic structure at both test temperatures, 25°C and 37°C. The heat-treated samples, on the other hand, exhibited basically an R-phase structure at 25°C and at 37°C. However, it is worth noting that at 37°C, they are in a region where it may be present little amounts of austenite.

It is worth noting that the tensile tests have shown that low levels of stress and deformation are required to induce martensite from the R-phase. In such case, it is likely that martensite is formed really soon on the fatigue cycles of HT samples in the region submitted to the maximum strain amplitudes, resulting in a local R-phase/martensitic structure that will support the majority of fatigue damage.

The different phases seem to influence deeply the strain controlled fatigue resistance: the R-phase/martensitic structure (400°C – 25°C) requires a much larger number of cycles to fail than the austenitic structure (AR – 25°C and 37°C). The AR sample

presented similar number of cycles to failure on both tested temperatures, which can be due to similar austenitic microstructures, while the structures containing austenite nuclei and R-phase/martensite (400°C – 37°C) have shown intermediate fatigue resistance.

Also, the increase in the test temperature is expected to increase the stability of the high-temperature phase, resulting in a higher level of stress required to induce the martensitic transformation. On the other hand, within this range of temperature, no significant effects are expected in the tensile strength. In this manner, plastic deformation and defect accumulation are facilitated, contributing to decreasing the number of cycles to failure at 37°C when compared to 25°C.

Before discussing the fatigue mechanism in each case, it is worth noting that low-cycle strain-controlled fatigue life is reported (2,13,23,24) to be controlled by crack propagation. In fact, the high flexural strain used on this study favors fast crack nucleation on regions of stress concentration such as surface defects and around inclusions, resulting in the multiple nucleation sites observed on the fracture surfaces in Figure 7.

Comparing the crack propagation in the two different microstructures, it is expected that martensitic induced transformation occurs on the crack tip of the austenitic superelastic AR wires, controlling the stable fatigue propagation of nucleated cracks. In the heat treated wires, on the other hand, the multiple variants of the R-phase and B19’ martensite in the region around the nucleated crack will give rise to a diversity of propagation paths at the variant boundaries, resulting in crack ramification and a large dissipation of energy during its propagation, as observed by Figueiredo et al, 2009 (13). Also, a local reorientation of martensite and R-phase around the cracks is expected to result in lower stress levels and stress concentration when compared to the AR wires, as reported in the literature (13,16,25). Thus, the crack breaching and the lower stress level and concentration can justify the larger number of cycles to failure observed in the heat-treated samples.

5.5. Conclusions

In this study, a heat treatment was performed at 400°C for 30 min in an initially superelastic near-equiatomic Ni-rich NiTi wire. The heat treated and the as-received

wires were characterized by XRD, DSC, tensile tests to rupture and loading/unloading and rotating/bending fatigue tests.

Wires in the as-received state were constituted by a strain hardened austenitic structure while in the heat-treated state, the R-phase was observed and the presence of Ti_3Ni_4 precipitates was inferred. The heat treatment resulted in an increase of the austenitic finishing transformation temperatures and in the ultimate tensile strengths, while the stress and deformation at the stress plateau decreased.

A significant fatigue resistance improvement at 4% maximum strain amplitude was obtained by the heat treatment. In this aggressive strain condition, cracks nucleated easily and fatigue life was controlled by crack propagation. This increase in fatigue resistance was associated to crack ramification and stress relief around the cracks in the initially R-phase microstructure.

The increase in the test temperature seems to result in a decrease in the fatigue life of the wires due to the increase in the stress required to induce martensite, moving its value closer to the ultimate tensile strength and, thus, facilitating the formation of local plastic deformation and increasing the generated defects.

Acknowledgements

This study was partially financed by the Coordenação de Aperfeiçoamento de Pessoal de Nível Superior - Brasil (CAPES) - Finance Code 001, Conselho Nacional de Desenvolvimento Científico e Tecnológico (CNPq) and the Fundação de Amparo à Pesquisa de Minas Gerais (FAPEMIG).

References

1. Otsuka K, Wayman CM. Shape Memory Materials. Cambridge. Cambridge University Press; 1998. 284 p.

2. Pelton AR. Nitinol Fatigue : A Review of Microstructures and Mechanisms. J Mater Eng Perform. 2011;20(July):613–7.

3. Wang Z, Zu X, Feng X, Dai J. Effect of thermomechanical treatment on the two-way shape memory effect of NiTi alloy spring. Mater Lett. 2002;54(May):55–61.

4. Feninat F El, Laroche G, Fiset M, Mantovani D. Shape Memory Materials for

Biomedical Applications. Adv Eng Mater. 2002;4(3):91–104.

5. Khalil-Allafi J, Dlouhy A, Eggeler G. Ni4Ti3-precipitation during aging of NiTi shape memory alloys and its influence on martensitic phase transformations. Acta Mater. 2002;50(17):4255–74.

6. Khalil-Allafi J, Behnam A-A. Multiple-step martensitic transformations in the Ni 51 Ti 49 single. J Mater Sci. 2010;45:6440–5.

7. Otsuka K, Ren X. Physical metallurgy of Ti – Ni-based shape memory alloys. Prog Mater Sci. 2005;50:511–678.

8. Duerig TW, Bhattacharya K. The Influence of the R-Phase on the Superelastic Behavior of NiTi. Shape Mem Superelasticity [Internet]. Springer International Publishing; 2015;1(2):153–61. Available from: http://link.springer.com/10.1007/s40830-015-0013-4

9. Shen Y, Zhou H, Zheng Y, Peng B, Haapasalo M. Current Challenges and Concepts of the Thermomechanical Treatment of Nickel-Titanium Instruments. J Endod [Internet]. Elsevier Ltd; 2013;39(2):163–72. Available from: http://dx.doi.org/10.1016/j.joen.2012.11.005

10. Kuhn G, Jordan L. Fatigue and Mechanical Properties of Nickel- Titanium Endodontic Instruments. J Endod. 2002;28(10):716–20.

11. Pereira ESJ, Viana ACD, Buono VTL, Peters OA, Bahia MG de A. Behavior of Nickel-Titanium Instruments Manufactured with Different Thermal Treatments. J Endod. 2015;41(1):67–71.

12. Eggeler G, Hornbogen E, Yawny A, Heckmann A, Wagner M. Structural and functional fatigue of NiTi shape memory alloys. Mater Sci Eng A. 2004;378(1-2 SPEC. ISS.):24–33.

13. Figueiredo AM, Modenesi P, Buono V. Low-cycle fatigue life of superelastic NiTi wires. Int J Fatigue [Internet]. Elsevier Ltd; 2009;31(4):751–8. Available from: http://dx.doi.org/10.1016/j.ijfatigue.2008.03.014

14. Santos LDA, Resende PD, Bahia MGDA, Buono VTL. Effects of R-Phase on Mechanical Responses of a Nickel-Titanium Endodontic Instrument: Structural

Characterization and Finite Element Analysis. Sci World J. 2016;2016.

15. Kim JI, Liu Y, Miyazaki S. Ageing-induced two-stage R-phase transformation in Ti - 50.9at.%Ni. Acta Mater. 2004;52(2):487–99.

16. Wang XB, Verlinden B, Van Humbeeck J. R-phase transformation in NiTi alloys. Mater Sci Technol [Internet]. 2014;30(13):1517–29. Available from: http://www.tandfonline.com/doi/full/10.1179/1743284714Y.0000000590

17. Sinha A, Mondal B, Chattopadhyay PP. Mechanical properties of Ti-(~49at%) Ni shape memory alloy, part II: Effect of ageing treatment. Mater Sci Eng A [Internet]. Elsevier; 2013;561:344–51. Available from: http://dx.doi.org/10.1016/j.msea.2012.10.023

18. Standard test method for tension testing of nickel-titanium superelastic materials. ASTM - F2516. 2015. p. 1–6.

19. Goryczka T, Morawiec H. Structure studies of the R-phase using X-ray diffraction methods. J Alloys Compd. 2004;367(1-2):137–41.

20. Helbert G, Saint-Sulpice L, Arbab Chirani S, Dieng L, Lecompte T, Calloch S, et al. Experimental characterisation of three-phase NiTi wires under tension. Mech Mater [Internet]. Elsevier Ltd; 2014;79:85–101. Available from: http://dx.doi.org/10.1016/j.mechmat.2014.07.020

21. Khalil-allafi J, Eggeler G, Dlouhy A, Schmahl WW, Somsen C. On the influence of heterogeneous precipitation on martensitic transformations in a Ni-rich NiTi shape memory alloy. Mater Sci Eng A. 2004;378:148–51.

22. Jiang F, Liu Y, Yang H, Li L, Zheng Y. Effect of ageing treatment on the deformation behaviour of Ti – 50 . 9 at .% Ni. Acta Mater [Internet]. Acta Materialia Inc.; 2009;57(16):4773–81. Available from: http://dx.doi.org/10.1016/j.actamat.2009.06.059

23. Braga LCM, Silva ACF, Buono VTL, Bahia MG de A. Impact of Heat Treatments on the Fatigue Resistance of Different Rotary Nickel-titanium Instruments. J Endod. 2014;40(9):7–10.

24. Pereira ESJ, Gomes RO, Leroy AMF, Singh R, Peters OA, Bahia MGA, et al.

Mechanical behavior of M-Wire and conventional NiTi wire used to manufacture rotary endodontic instruments. Dent Mater. 2013;29:e318–24.

25. Alarcon E, Heller L, Chirani SA, Šittner P, Kopeček J, Saint-Sulpice L, et al. Fatigue performance of superelastic NiTi near stress-induced martensitic transformation. Int J Fatigue. 2017;95:76–89.

6. EFFECT OF PHASE CONSTITUTION IN LOW-CYCLE FATIGUE OF NiTi WIRES

Jéssica Dornelas Silva*, Natalia Isabel de Azevedo Lopes, Pedro Damas Resende, Leandro de Arruda Santos, Vicente Tadeu Lopes Buono

Department of Metallurgical and Materials Engineering, Universidade Federal de Minas Gerais (UFMG), Belo Horizonte, MG, Brazil

*Corresponding author: jdornelassilva@gmail.com

Abstract

Vastly used due to their functional properties, NiTi shape memory alloys have mechanical properties and fatigue resistance known to be strongly affected by their thermomechanical state. In this work, the goal was to evaluate the fatigue resistance of near equiatomic Ni-rich NiTi heat treated wires in different test temperatures. In this manner, it was possible to evaluate the microstructure effect on the fatigue resistance with a fixed thermomechanical condition. For that, a heat treatment at 500°C for 30 min was performed in initially superelastic wires in an argon atmosphere. DSC tests were performed in order to obtain the transformation temperatures and there different fatigue test temperatures were chosen according to the phase stability ranges. Rotating-bending fatigue tests were performed in proper equipment at 4% maximum strain, evaluating the R-phase, austenitic and R-phase + austenitic structures properties according to the selected test temperatures. The results showed that the R-phase presents higher low-cycle fatigue resistance than austenite and a fatigue mechanism was proposed.

Keywords: nickel-titanium alloys; shape memory; superelasticity; microstructure, fatigue resistance.

6.1. Introduction

Near equiatomic NiTi alloys are attractive shape memory alloys due to the combination of their mechanical properties with their functional capabilities, being suitable to a wide range of engineering and medical applications (1). Within these applications, NiTi wires are commonly subjected to fluctuating stresses and strains, being prone to failure by fatigue. The fatigue resistance of these alloys depends on the microstructure, the

transformation temperatures and on the thermomechanical state. But its complex structure and structure variations with the heat treatment parameters and the thermomechanical history make fatigue behavior hard to understand and to predict (2–5).

In this context, recent studies have been made to evaluate some microstructural effects on the crack growth and fatigue life such as the effect of downsizing inclusions (6), grain size (7) and grain orientation around stress concentrators (8) as well as attempts to obtain analytical models to describe the non-linear fatigue behavior of these materials (9,10). In the present study, the goal is to evaluate the effect of the different phases on the fatigue NiTi wires with a fixed thermomechanical history. For this purpose, fatigue tests were performed at different temperatures for wires in the same initial condition.

6.2. Experimental procedure

The material used on this study was a 1mm diameter 51%Ni-49%Ti superelastic wire heat-treated at 500°C in a tubular furnace with an argon controlled-atmosphere for 30 min and then water cooled.

The heat-treated wires were firstly characterized at room temperature by means of X-ray diffractometry (XRD) analyses and tensile tests. The XRD tests were performed in with 2θ ranging from 30° to 120° for phase identification using Cu-Kα (λ = 0.15418 nm) radiation and a scan speed of 0.02°/s. The peaks were identified by comparison with patterns from the ICSD database and spectra available in the literature (11–14).

The tensile tests took place in an Instron 5582 testing machine in order to evaluate the mechanical behavior of the wires. In accordance to ASTM F2516−14 standard (15), tests until rupture were performed at a crosshead speed of 12 mm/min and loading and unloading up to 6% deformation at a crosshead speed of 1.2 mm/min. The experiments were repeated three times.

Differential scanning calorimetry was performed to determinate the direct and reverse martensitic transformation temperatures and, thus, the phase stability range in a Shimadzu DSC-60 calorimeter at a cooling/heating rate of 10°C from -100°C to 100°C. The tests were performed in triplicate by cooling each specimen from room temperature to -100°C, following by heating to 100°C, cooling it back to -100°C and heating to room temperature. The reverse transformation temperatures were determined in the

interval from -100°C to 100°C, while the direct ones on the subsequent cooling step. Then, the fatigue test temperatures were selected in order to evaluate the wire's performance with different stable phases.

The fatigue tests took place in proper flexural fatigue machine at 4% maximum strain in water baths at the chosen temperatures. The fractured surfaces were analyzed in an FEI – Inspect 550 scanning electron microscope (SEM) operating at 15kV using secondary electrons.

6.3. Results

The R-phase was identified in the XRD analysis of the heat treated sample, characterized in Figure 1(11,16) . The presence of the coherent precipitates Ti_3Ni_4 could also be observed (17).

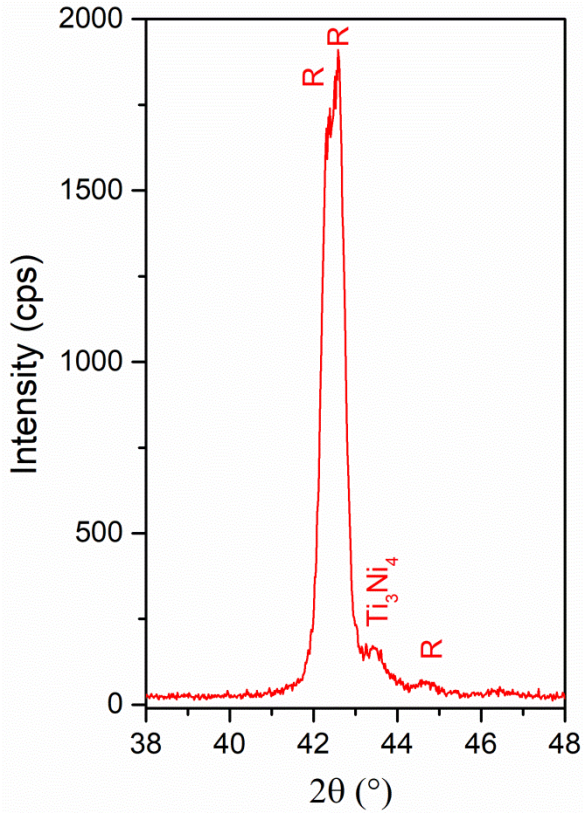

Figure 6.1 – Characteristic R-phase peaks observed in the XRD analysis of the heat-treated alloy at room temperature.

The mechanical behavior in the performed tensile tests is presented in Figure 2. In the rupture curve, represented as a full line, the stress plateau was reached at around 350MPa and a strain of around 6% was achieved. A mean rupture stress of 1280MPa

was observed with a deviation smaller than 2%. In the loading/unloading curve, represented as a dashed line, the stress at which the plateau is reached is around 300MPa. The difference between this value obtained from the rupture curve and the loading/unloading curve can be explained by the different strain rates used in each test. Moreover, a large residual strain was observed during unloading and a full shape recovery could be achieved by heating.

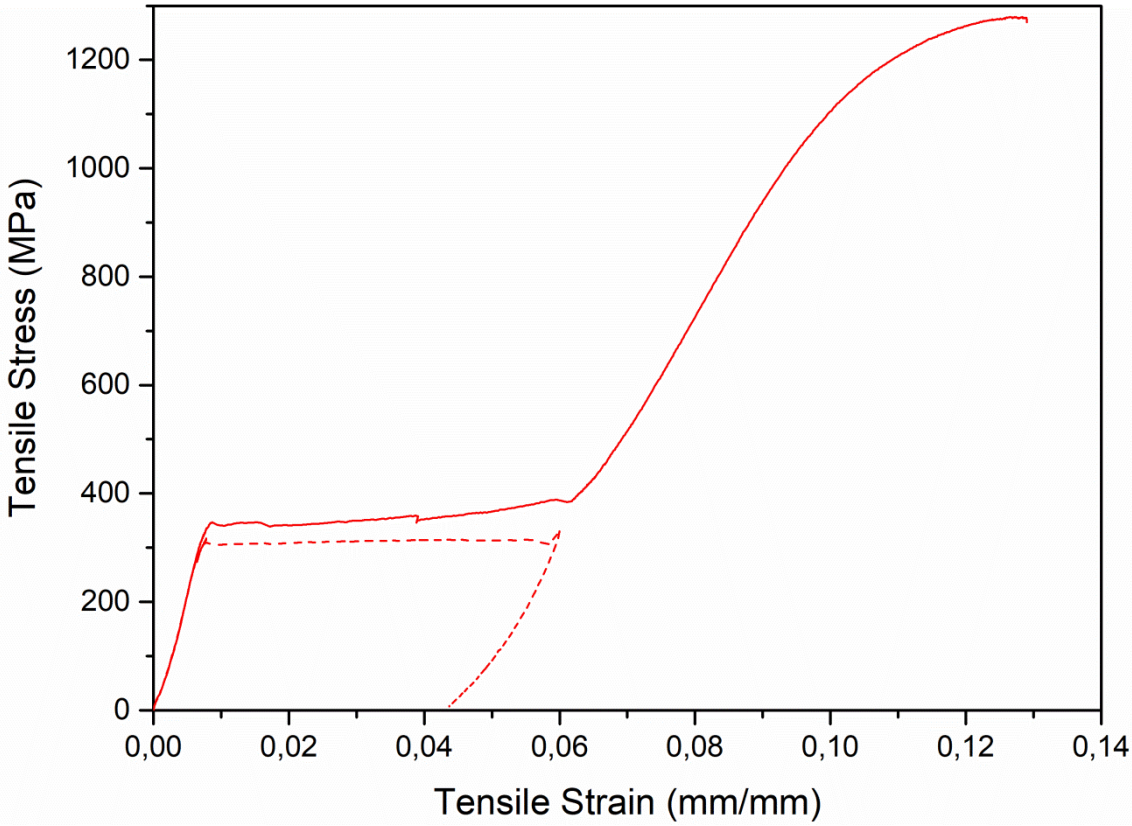

Figure 6.2 – Representative tensile stress x strain rupture (full line) and loading/unloading curves (dashed line) obtained in the tension test of the heat-treated sample at room temperature.

Figure 3 presents the obtained DSC chart. Two peaks were detected during cooling and during heating, characterizing a symmetric R-phase transformation (18). Martensitic transformations involving the R-phase are common on heat treated samples. The R-phase is a pre-martensitic trigonal phase that involves lattices distortions much smaller than the martensitic direct transformations. The coherent precipitates formed during the heat treatment generate lattice distortions that favor the R-phase formation and, thus, two-step transformations (19).

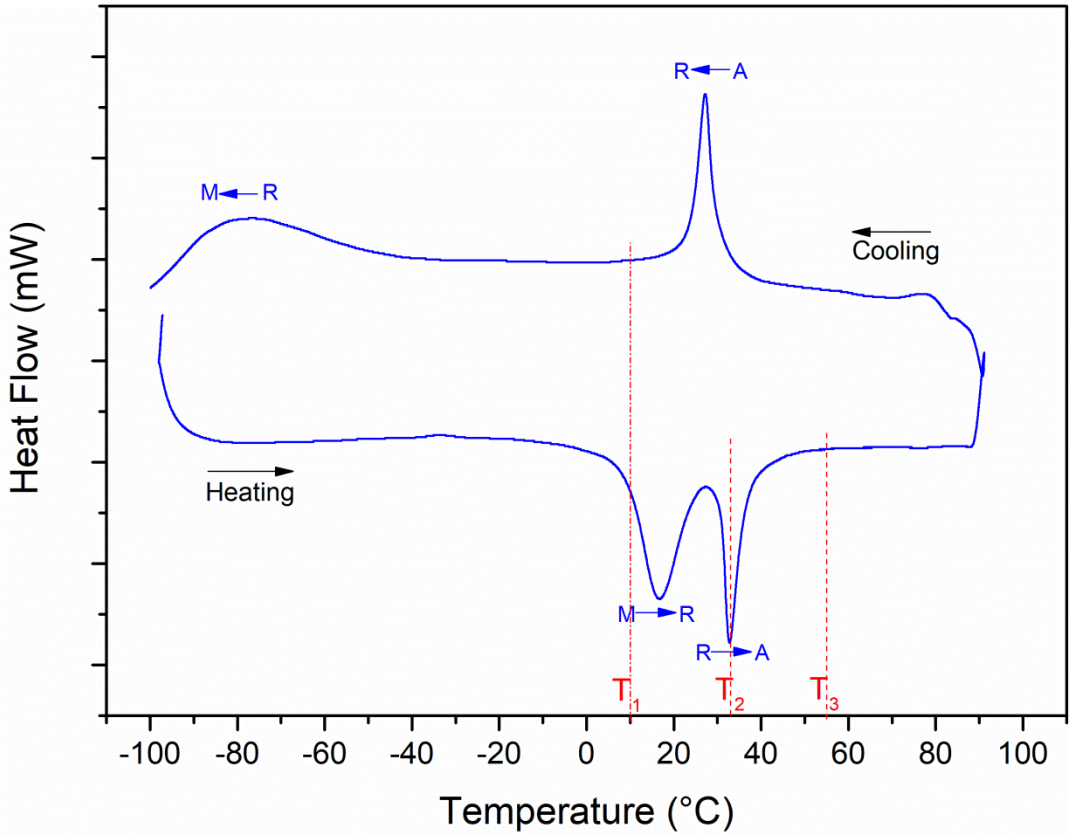

Figure 6.3 – DSC chart obtained for the heat treated wire, where the selected fatigue test temperatures T_1,T_2 and T_3 are highlighted.

In this manner, the detected peaks are identified on the chart. During cooling, the first peak refers to an austenite (A) -> R-phase (R) transformation and the second to the R-phase (R) -> martensite (M) transformation. During heating, the first peak refers to an M->R transformation and the second, to an R->A transformation. Note that there is a small hysteresis between the R-A transformations during cooling and heating and that these peaks have a characteristic sharp profile like pointed out by Wang, 2014(13).

Considering the heat-treated wires are kept at room temperature (~22°C), three different temperatures were selected to perform the fatigue tests and are presented in Table 1. T_1 is in an R-phase region on the cooling curve, T_3, in an austenitic region and T_2, in a two-phase austenitic + R-phase region on the heating curve.

Table 6.1 – Temperatures selected after de DSC analyses for the fatigue test and the respective microstructures.

	Temperature	Microstructure
T_1	10°C	R-phase
T_2	33°C	R-phase + Austenite
T_3	55°C	Austenite

The mean numbers of cycles to failure in each temperature are presented in Figure 4. The highest fatigue life was observed on the R-phase (10°C) and the lowest, on the austenite (55°C). The two-phase structure at 33°C presented an intermediate behavior.

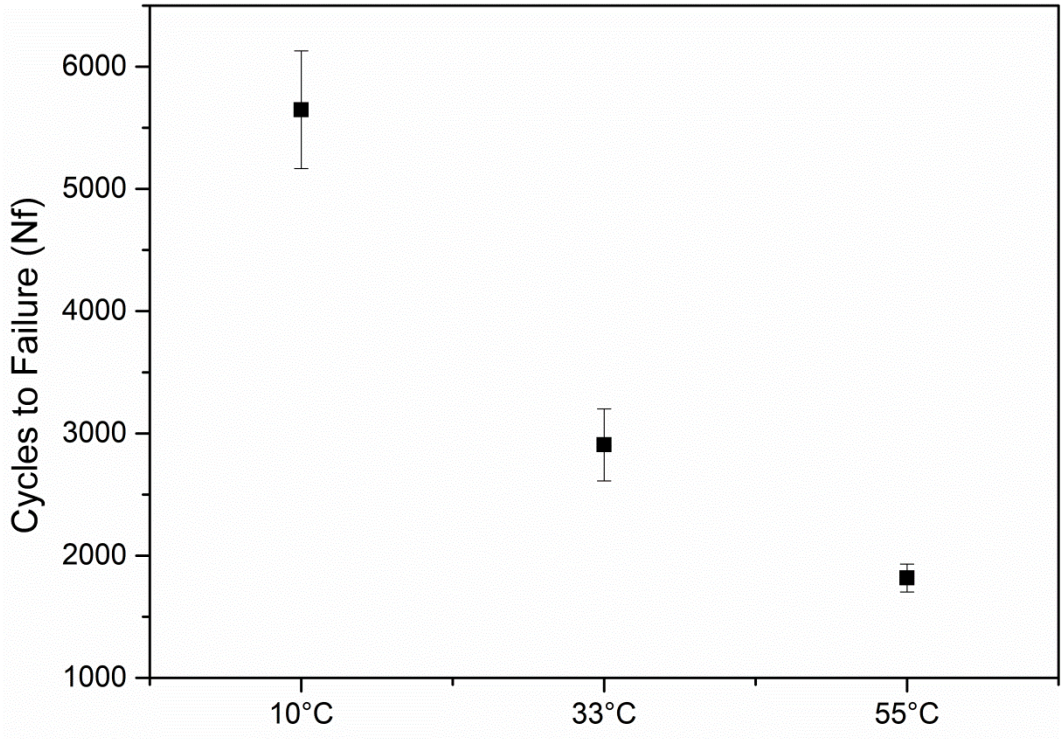

Figure 6.4 – Mean number of cycles to failure at 4% maximum strain fatigue tests according to the test temperature.

The fracture surfaces of the fatigue tested samples (Figure 5) presented two different regions: a slow fatigue crack propagation region and a ductile final rupture region. Between these two regions, a transition zone could be observed. While the fatigue region, in detail in Figure 5 (b, e and h), is characterized by the presence of fatigue striations, the ductile fracture region, in detail in Figure 5 (c, f and i) is characterized by the presence of dimples. In Figure 5 (b, e and h), it is possible to see that the striation spacing and the number of cracks through them increase with increasing temperature. It is also possible to notice in Figure 5 (a, d and g) that the fraction of area occupied by the ductile area increases when the Nf decreases. Also, multiple crack nucleation sites can be pointed, as indicate by arrows**.**

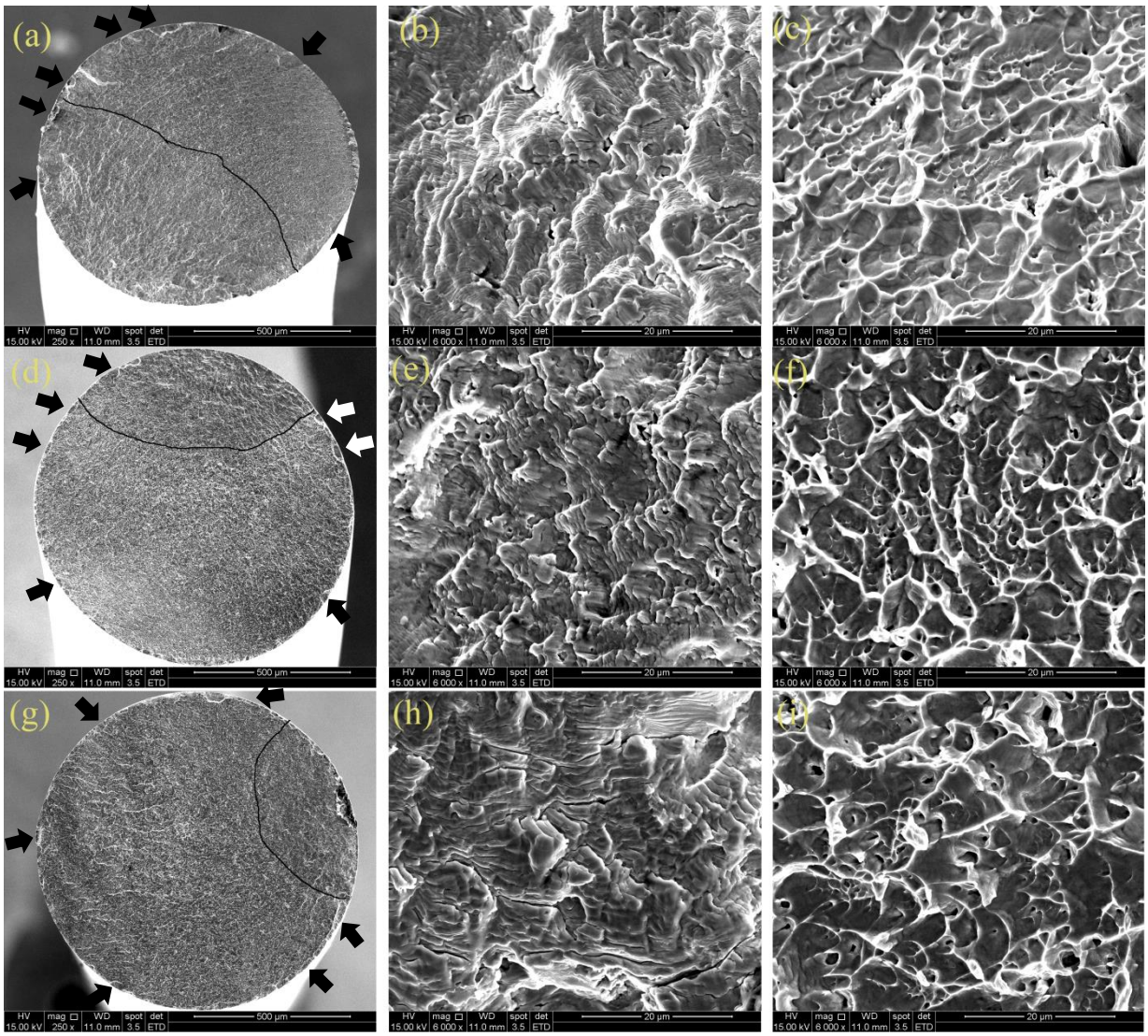

Figure 6.5 – Fracture analysis of the fatigue test samples at (a), (b) and (c) 10°C; (d), (e) and (f) 33°C; and (g), (h) and (i) 55°C.

It is worth noting that microcracks could be observed through the striations in the slow propagation area of the samples tested at 33°C and 55°C, as it can be noted in Figure 6. These types of microcracks were not observed in the samples tested at 10°C.

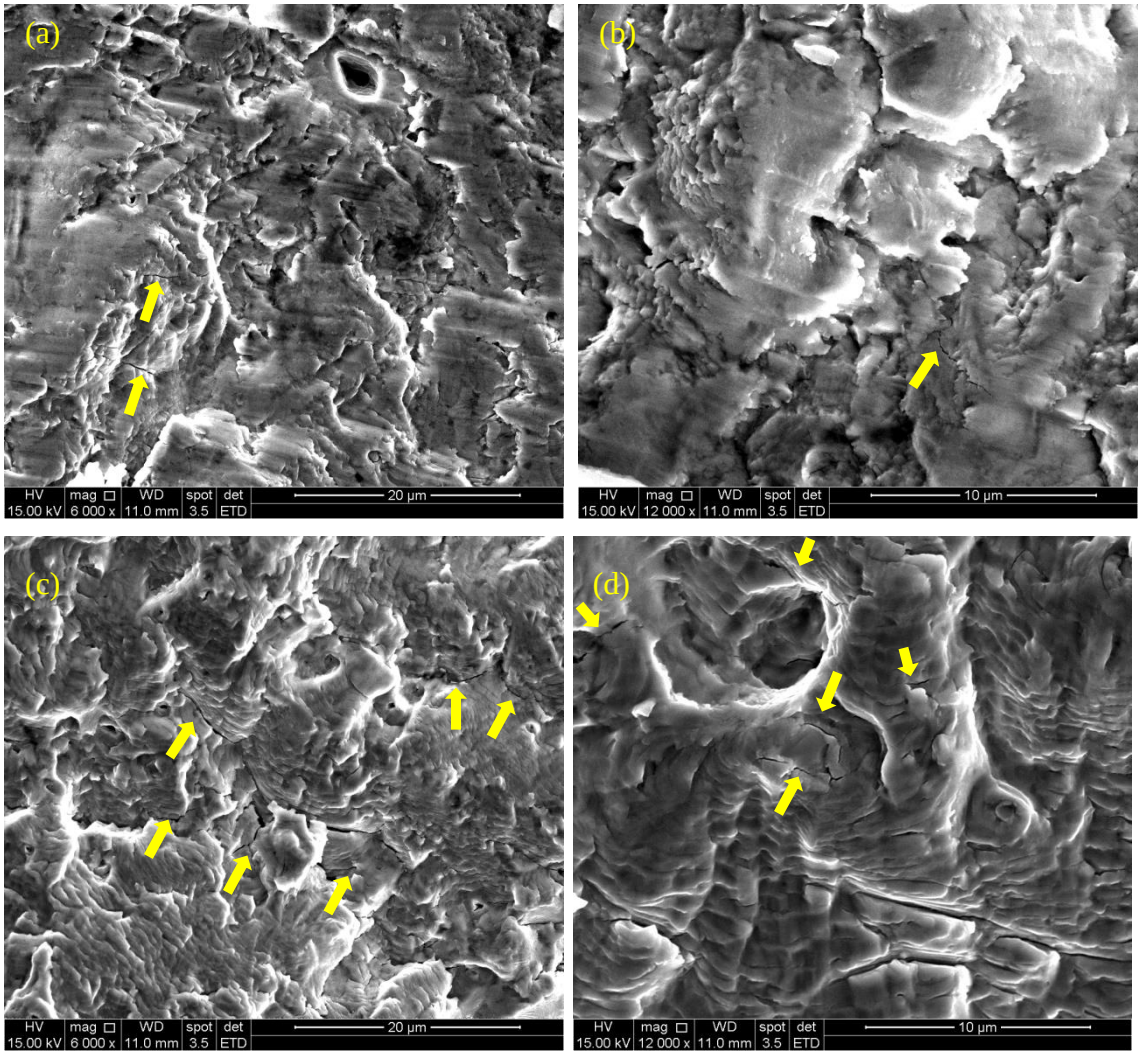

Figure 6.6 – Microcracks observed in the slow crack propagation region in samples tested at (a) and (b) 33°C and (c) and (d) 55°C.

6.4. Discussion

The highest number of cycles to failure was obtained at 10°C, in the R-phase structure and the lowest, at 55°C, in the austenitic structure, which indicates that the fatigue resistance at 4% strain of stable R-phase structure is much higher than for an austenitic structure. A biphasic structure presented intermediate fatigue resistance.

During cycling in a fatigue regime, cracks nucleate on stress concentration regions and go through a process of growing and blunting up until a point where the predominant

crack reaches a critical size and propagates unstably, causing the component's fracture. In high stress/strain amplitudes, the crack propagation is an important aspect on the fatigue resistance, since it prevails in the fatigue life (20–23).

In fact, low-cycle fatigue in NiTi alloys is reported (24–26) to be controlled by crack propagation. The aggressive strain amplitude in which the wires are subjected favors the fast crack nucleation, as it can be related to the various fatigue initiation sites along the fracture surfaces in Figure 5, making crack propagation predominant on the fatigue life.

Thus, the results obtained from this study lead to the conclusion that crack propagation through the R-phase requires amounts of energy higher than at the austenite. This is evidenced by the smaller fraction of ductile area in the R-phase microstructure and the smaller striation spacing.

Unlike in conventional materials, the crack propagation in low-cycle fatigue of NiTi seems to be deeply related to the martensitic induced transformation rather by the existence of a plastic region around the crack tip (27,28). In both microstructures, the induced martensitic transformation is expected to occur during loading on cycling but while the reverse transformation occurs during unloading in the austenite, it probably does not occur in the R-phase, as it was observed in the tensile tests at room temperature in Figure 2.

On one hand, the induced martensitic from austenite is reported (29–31) to be associated with a high amount of dislocations generated. In fact, the high amount of microcracks through the striations in the samples tested at 55°C and 33°C (Figure 5-h and Figure 6) can be related to a local stress concentration due to the dislocations generated during the induced and reverse martensitic transformation.

On the other hand, the R-phase/martensitic structure is associated with a high density of interfaces among the variants. In these aspects, while the crack propagates generating a high amount of defects on the crack tip and along the wire where induced martensitic transformation occurs, on the R-phase/martensite, the interfaces give the crack multiple paths to propagate, inducing crack branching like observed by Figueiredo, 2009 (5).

The crack branching along the variant interfaces results in high energy dispersion during propagation in the R-phase, being related to the high number of cycles to failure spent during fatigue propagation. This is evidenced by the fine striation spacing at 10°C and

the relative size of the fatigue/ductile areas: the fine striation spacing is related to relatively small increments on the fatigue crack size during cycling and the smaller ductile area is related to higher fatigue toughness.

Conclusions

In this paper, bending-rotating fatigue tests at 4% maximum strain were performed at different temperatures in NiTi heat-treated wires: 10°C, 33°C and 55°C. At 10°C, the wires are expected to be constituted by the R-phase, at 33°C, by a two-phase austenitic + R-phase structure, and at 55°C, by austenite. The highest number of cycles to failure was obtained on the R-phase structure, which can be related both to a high energy dispersion during propagation on the R-phase and to the high amount of defects associated with the martensitic induced transformation in the austenitic state.

Acknowledgements

This study was partially financed by the Coordenação de Aperfeiçoamento de Pessoal de Nível Superior - Brasil (CAPES) - Finance Code 001, Conselho Nacional de Desenvolvimento Científico e Tecnológico (CNPq) and the Fundação de Amparo à Pesquisa de Minas Gerais (FAPEMIG).

References

1. Otsuka K, Wayman CM. Shape Memory Materials. Cambridge. Cambridge University Press; 1998. 284 p.

2. Kollerov M, Lukina E, Gusev D, Mason P, Wagstaff P. Impact of material structure on the fatigue behaviour of NiTi leading to a modified Coffin-Manson equation. Mater Sci Eng A [Internet]. Elsevier; 2013;585:356–62. Available from: http://dx.doi.org/10.1016/j.msea.2013.07.072

3. Pelton AR. Nitinol Fatigue : A Review of Microstructures and Mechanisms. J Mater Eng Perform. 2011;20(July):613–7.

4. Khalil-allafi J, Eggeler G, Dlouhy A, Schmahl WW, Somsen C. On the influence of heterogeneous precipitation on martensitic transformations in a Ni-rich NiTi shape memory alloy. Mater Sci Eng A. 2004;378:148–51.

5. Figueiredo AM, Modenesi P, Buono V. Low-cycle fatigue life of superelastic

NiTi wires. Int J Fatigue [Internet]. Elsevier Ltd; 2009;31(4):751–8. Available from: http://dx.doi.org/10.1016/j.ijfatigue.2008.03.014

6. Coda A, Cadelli A, Zanella M, Fumagalli L. Straightforward Downsizing of Inclusions in NiTi Alloys: A New Generation of SMA Wires with Outstanding Fatigue Life. Shape Mem Superelasticity [Internet]. Springer International Publishing; 2018;4(1):41–7. Available from: http://link.springer.com/10.1007/s40830-018-0159-y

7. Lepage WS, Ahadi A, Lenthe WC, Sun QP, Pollock TM, Shaw JA, et al. Grain size effects on NiTi shape memory alloy fatigue crack growth. J Mater Res. 2018;33(2):91–107.

8. Paul PP, Fortman M, Paranjape HM, Anderson PM, Stebner AP, Brinson LC. Influence of Structure and Microstructure on Deformation Localization and Crack Growth in NiTi Shape Memory Alloys. Shape Mem Superelasticity [Internet]. Springer International Publishing; 2018;1–9. Available from: http://link.springer.com/10.1007/s40830-018-0172-1

9. Allegretti D, Francesca Berti B, Francesco Migliavacca B, Giancarlo Pennati B, Petrini L. Fatigue Assessment of Nickel–Titanium Peripheral Stents: Comparison of Multi-Axial Fatigue Models. Shape Mem Superelasticity [Internet]. Springer International Publishing; 2018;4(1):186–96. Available from: https://doi.org/10.1007/s40830-018-0150-7

10. Vantadori S, Carpinteri A, Di Cocco V, Iacoviello F, Natali S. Fatigue analysis of a near-equiatomic pseudo-elastic NiTi SMA. Theor Appl Fract Mech [Internet]. Elsevier; 2018;94(January):110–9. Available from: https://doi.org/10.1016/j.tafmec.2018.01.012

11. Santos LDA, Resende PD, Bahia MGDA, Buono VTL. Effects of R-Phase on Mechanical Responses of a Nickel-Titanium Endodontic Instrument: Structural Characterization and Finite Element Analysis. Sci World J. 2016;2016.

12. Kim JI, Liu Y, Miyazaki S. Ageing-induced two-stage R-phase transformation in Ti - 50.9at.%Ni. Acta Mater. 2004;52(2):487–99.

13. Wang XB, Verlinden B, Van Humbeeck J. R-phase transformation in NiTi

alloys. Mater Sci Technol [Internet]. 2014;30(13):1517–29. Available from: http://www.tandfonline.com/doi/full/10.1179/1743284714Y.0000000590

14. Sinha A, Mondal B, Chattopadhyay PP. Mechanical properties of Ti-(~49at%) Ni shape memory alloy, part II: Effect of ageing treatment. Mater Sci Eng A [Internet]. Elsevier; 2013;561:344–51. Available from: http://dx.doi.org/10.1016/j.msea.2012.10.023

15. Standard test method for tension testing of nickel-titanium superelastic materials. ASTM - F2516. 2015. p. 1–6.

16. Mohri M, Taghizadeh M, Wang D, Hahn H, Nili-Ahmadabadi M. Microstructural study and simulation of intrinsic two-way shape memory behavior of functionally graded Ni-rich/NiTiCu thin film. Mater Charact [Internet]. Elsevier; 2018;135(August 2017):317–24. Available from: https://doi.org/10.1016/j.matchar.2017.11.056

17. Prokofiev EA, Burow JA, Payton EJ, Zarnetta R, Frenzel J, Gunderov D V., et al. Suppression of Ni4Ti3 precipitation by grain size refinement in Ni-rich NiTi shape memory alloys. Adv Eng Mater. 2010;12(8):747–53.

18. Duerig TW, Bhattacharya K. The Influence of the R-Phase on the Superelastic Behavior of NiTi. Shape Mem Superelasticity [Internet]. Springer International Publishing; 2015;1(2):153–61. Available from: http://link.springer.com/10.1007/s40830-015-0013-4

19. Otsuka K, Ren X. Physical metallurgy of Ti – Ni-based shape memory alloys. Prog Mater Sci. 2005;50:511–678.

20. Fine ME, Chung Y-W. Fatigue Failure in Metals. ASM HANDBOOK - Fatigue and Fracture. ASM International; 1996.

21. Meyers MA, Chawla KK. Mechanical Behavior of Materials [Internet]. 2nd ed. Cambridge University Press; 2009. 882 p. Available from: http://www.smesfair.com/pdf/mechanical eng/smesfair09.pdf

22. ASM International. Fatigue. Elements of Metallurgy and Engineering Alloys. 2008. p. 243–65.

23. Dieter GE. Mechanical Metallurgy. Nova York: McGraw-Hill Book Company; 1961.

24. Bahia MG de A, Dias RF, Buono VT. The influence of high amplitude cyclic straining on the behaviour of superelastic NiTi. Int J Fatigue. 2006;28(9):1087–91.

25. Robertson SW, Pelton AR, Ritchie RO. Mechanical fatigue and fracture of Nitinol. Int Mater Rev [Internet]. 2012;57(1):1–37. Available from: http://www.tandfonline.com/doi/full/10.1179/1743280411Y.0000000009

26. Sawaguchi T, Kaustrater G, Yawny A, Wagner M. Crack Initiation and Propagation in 50.9 At . pct Ni-Ti Pseudoelastic Shape-Memory Wires in Bending-Rotation Fatigue. Metall Mater Transations A. 2003;34(December):2847–60.

27. Di Cocco V, Iacoviello F, Maletta C, Natali S. Cyclic microstructural transitions and fracture micromechanisms in a near equiatomic NiTi alloy. Int J Fatigue [Internet]. Elsevier Ltd; 2014;58:136–43. Available from: http://dx.doi.org/10.1016/j.ijfatigue.2013.03.009

28. Gollerthan S, Young ML, Baruj A, Frenzel J, Schmahl WW, Eggeler G. Fracture mechanics and microstructure in NiTi shape memory alloys. Acta Mater [Internet]. Acta Materialia Inc.; 2009;57(4):1015–25. Available from: http://dx.doi.org/10.1016/j.actamat.2008.10.055

29. Delville R, Malard B, Pilch J, Sittner P, Schryvers D. Transmission electron microscopy investigation of dislocation slip during superelastic cycling of Ni-Ti wires. Int J Plast [Internet]. Elsevier Ltd; 2011;27(2):282–97. Available from: http://dx.doi.org/10.1016/j.ijplas.2010.05.005

30. Alarcon E, Heller L, Chirani SA, Šittner P, Kopeček J, Saint-Sulpice L, et al. Fatigue performance of superelastic NiTi near stress-induced martensitic transformation. Int J Fatigue. 2017;95:76–89.

31. Heller L, Seiner H, Šittner P, Sedlák P, Tyc O, Kadeřávek L. On the plastic deformation accompanying cyclic martensitic transformation in thermomechanically loaded NiTi. Int J Plast. 2018;(February).

7. CONSIDERAÇÕES FINAIS

Neste estudo, tratamentos térmicos em diferentes temperaturas foram realizados em fios de NiTi inicialmente superelásticos, de composição aproximadamente equiatômica com um pequeno excesso de Ni e os efeitos destes tratamentos na resistência à fadiga foram estudados. As seguintes conclusões podem ser apontadas.

Por meio de análises das propriedades mecânicas e das temperaturas de transformação nos fios tratados, em conjunto com as análises de difratometria de raios X, permitiram inferir que os tratamentos térmicos a 300°C e 350°C promoveram a recuperação da austenita inicialmente encruada. Tratamentos térmicos entre 400°C e 600°C promoveram a precipitação de partículas ricas em Ni. Em temperaturas mais baixas neste intervalo, geralmente formam-se precipitados coerentes de Ti_3Ni_4. Mudanças nas temperaturas de transformação e na tensão limite de resistência indicam que houve aumento no tamanho e na quantidade desses precipitados com o aumento da temperatura de tratamento. Em 600°C, as mudanças em propriedades mecânicas indicam que precipitados não coerentes foram formados e ocorreu a recristalização da matriz austenítica.

Dentre os fios tratados termicamente no intervalo de 300°C a 600°C, os fios resultantes dos tratamentos de 400°C e 450°C apresentaram as maiores resistências à fadiga por flexão em 4% de deformação máxima na temperatura de ensaio de 37°C. Nestes fios, a fase R era predominante tanto à temperatura ambiente quanto na temperatura de ensaio.

Os tratamentos térmicos que tiveram destaque nos ensaios de fadiga (400°C e 450°C) foram repetidos e curvas deformação máxima em flexão (ε) vs número de ciclo para falha (N) foram obtidas à 37°C no intervalo de 1% a 5% de deformação. Nestes tratamentos, foram produzidos fios que apresentaram microestruturas bifásicas na temperatura de ensaio, constituídos por frações distintas de fase R e austenita. Pôde-se observar que dentre as deformações analisadas, ocorreu uma brusca mudança de regime entre 1% e 3% de deformação, reduzindo-se drasticamente o número de ciclos para a falha em ambos os casos. Ainda assim, comparando-se o número de ciclo para falha dos fios produzidos com fios NiTi em outras condições apresentados na literatura, nota-se que a resistência à fadiga obtida é considerável. Observou-se também que a resistência à

fadiga dos fios nessas duas condições estudadas não apresenta diferença estatisticamente significativa para 95% de confiança. Dessa forma, pode-se afirmar que tratamentos térmicos de fios superelásticos realizados entre estas duas temperaturas são recomendados para a obtenção de microestruturas resistentes à fadiga.

Ao se comparar os fios no estado como recebido com os fios tratados à 400°C em ensaios à 25°C e 37°C, mantendo-se a mesma microestrutura em cada fio em ambas as temperaturas, pôde-se perceber que temperatura tem efeitos na resistência à fadiga, em especial quando a fase predominante é a fase R. Este efeito foi relacionado ao fato de que em temperaturas mais baixas, menores tensões são necessárias para induzir a formação de martensita enquanto o limite de resistência não sofre grandes influências entre as duas temperaturas estudadas. Desta forma, a 37°C, quando a tensão necessária para induzir a formação e martensita é maior, mecanismos de deformação plástica localizada e de acúmulos de defeitos ocorrem mais facilmente, contribuindo para a diminuição do número de ciclos para falha quando comparado a 25°C.

Notou-se também que, enquanto os fios no estado como recebido são superelásticos, os fios tratados a 400°C apresentaram uma grande deformação residual após passarem por um ensaio de carregamento até 6% de deformação em tração seguido de descarregamento. Os fios tratados, que podem ter a forma recuperada por meio de um aquecimento moderado, apresentaram uma estrutura constituída por martensita e fase R após o descarregamento. Este é um indício que a martensita induzida durante o carregamento do fio incialmente constituído por fase R passa apenas por uma transformação reversa parcial de martensita para fase R no descarregamento, ao contrário dos fios austeníticos que passam por uma transformação reversa total.

Por fim, após tratar fios de NiTi à 500°C, realizou-se ensaios de fadiga por flexão a 4% de deformação máxima em temperaturas distintas, partindo-se de fios com a mesma condição inicial. Desta vez, as temperaturas foram selecionadas visando-se realizar ensaios em uma estrutura completamente austenítica, uma estrutura constituída por fase R e uma estrutura contendo estas duas fases. Observou-se que a fase R apresenta a maior resistência à fadiga nestas condições, a fase austenítica, a menor e a estrutura bifásica apresentou uma resistência intermediária.

Com a realização deste estudo, foi possível propor que a melhoria da resistência à fadiga em ligas tratadas de NiTi se deve à:

- Nas condições agressivas de deformações cíclicas analisadas, trincas se nucleiam facilmente na superfície dos fios, bem como ao redor de inclusões e outros defeitos, de forma que a vida em fadiga é controlada pela propagação de trincas.
- A fase R é uma fase pré-martensita constituída por variantes que dão às trincas nucleadas uma variedade de caminhos tortuosos para sua propagação entre seus contornos, resultando em trincas ramificadas e em um grande dispêndio de energia;
- A transformação induzida de fase R para martensita requer menores níveis de tensão, podendo ocorrer ao redor das trincas como uma forma de alívio de tensões;
- A transformação martensitica induzida a partir da austenita, assim como a transformação reversa, está associada a uma grande quantidade de defeitos produzidos durante a ciclagem mecânica, resultando na formação de regiões de maior concentração de tensão e nucleação de novas microtrincas, conforme observado em análises fractográfica;
- A transformação martensita induzida a partir da fase R não ocorre de maneira reversa, de forma que se espera que uma estrutura constituída por fase R + martensita suporte a maior parte do número de ciclos. Nesse caso, a não ocorrência da transformação reversa pode acarretar um menor número de defeitos gerados durante a ciclagem.

FINAL CONSIDERATIONS

In this study, heat-treatments in different temperatures were performed in Ni-rich near equiatomic NiTi superelastic wires and the effects of these treatments on the fatigue resistance were evaluated. The following conclusions were discussed.

By analyzing the mechanical properties and the transformation temperatures of the heat treated wires along with the XRD data, it was possible to infer that heat-treatments at 300°C and 350°C promoted the recovery process on the initially hardened austenite. Heat-treatments from 400°C to 600°C promoted the precipitation of Ni-rich particles. In lower temperatures within this range, coherent Ti_3Ni_4 are usually formed. Changes in the transformation temperature and in the ultimate tensile strength indicate that the size and the amount of precipitates increase with increasing heat-treatment temperature. In the 600°C heat-treatment, changes in the mechanical properties indicate that incoherent precipitates were formed and that the austenitic matrix went through recrystallization.

Among the wires heat-treated in the range of 300°C to 600°C, the wires that presented the highest fatigue resistance in strain-controlled flexural fatigue tests at 4% maximum strain at 37°C were the ones treated at 400°C and 450°C. In these wires, the R-phase was the predominant phase both at room temperature and test temperature.

The heat treatments that resulted in the best fatigue improvement (400°C and 450°C) were repeated and maximum flexural strain (ε) vs the number of cycles to failure (N) curves were obtained at 37°C in the range of 1% to 5% strain. In these treatments, wires that presented a microstructure constituted by different fractions of austenite + R-phase in the test temperature were obtained. Within the analyzed strain range, an abrupt change of fatigue behavior was observed within 1% and 3% deformation, where the number of cycles to failure dropped drastically in both cases. Still, comparing the fatigue life of the produced NiTi wires with ones in other conditions in the literature, the fatigue resistance obtained was considerably noticeable. It was also pointed out that the fatigue resistance in both studied conditions presented differences statistically negligible, in a manner that heat-treatments within this range of temperature are recommended for obtaining fatigue resistant microstructures.

By comparing wires in the as-received condition with wires heat-treated at 400°C in fatigue tests at 25°C and 37°C, maintaining the same microstructure in each condition in both test temperatures, it was observed that the temperature has effects on the fatigue resistance, especially when the R-phase is predominant. This effect was related to the fact that in lower temperatures, lower stresses are required to induce the martensitic transformation while the ultimate tensile strength does not suffer big effects in these two studied temperatures. In such way, at 37°C, when the stress required to induce the formation of martensite is higher, localized plastic deformation and defect accumulation mechanisms are facilitated, contributing for the decrease of the number of cycles to failure when compared to the samples tested at 25°C.

It was also noticed that, while wires in the as-received condition presented a superelastic behavior, the wires heat-treated at 400°C presented high residual strain after being loaded up to 6% strain in tension and unloaded to null load. The heat-treated wires, which could have the shape recovered by moderate heating, presented a microstructure constituted by martensite and R-phase after unloading. This is evidence that the martensite induced while loading the initially R-phase wire goes through only a partial reverse transformation during unloading, unlike the austenitic wires which go through a total reverse transformation.

Finally, after heat-treating wires at 500°C, flexural fatigue tests at 4% maximum strain were performed in distinct temperatures with a fixed initial wire condition. This time, the temperatures were selected aiming to perform tests in a completely austenitic structure, a completely R-phase structure and in a structure constituted by both of these phases. These tests showed that the R-phase presents the highest fatigue strength in the tested condition, the austenite, the lowest and the biphasic structure presented intermediate resistance.

By fulfilling this study, it was possible to propose that the improvement of the fatigue resistance in NiTi heat-treated alloys is due to:

- In the aggressive cyclic strain conditions analyzed, cracks nucleate easily in the wire’s surface as well as around inclusions in such a way that the fatigue life is controlled by crack propagation;

- The R-phase is a pre-martensitic phase constituted by variants between which the nucleated cracks have a variety of tortuous paths possible, resulting in crack ramification and in high energy spent;
- The induced transformation from the R-phase to martensite requires lower levels of stress, possibly occurring around the cracks as a way of stress relieving.
- The martensitic transformation induced by austenite, as well as the reverse transformation, is associated with a high amount of defects produced during mechanical cycling, resulting in the formation of stress concentration regions and the nucleation of new microcracks as observed in the fractographic analysis;
- The reverse martensitic induced transformation from the R-phase does not occur in such a way that a structure constituted by the R-phase and martensite is expected to bear the majority of the cycles. The non-occurrence of reverse transformation may implicate in lower amounts of defects generated during cycling.

SUGESTÕES PARA TRABALHOS FUTUROS

Para dar continuidade a este trabalho, sugere-se que sejam feitas análises de microscopia eletrônica de transmissão em fios termicamente tratados para a observação de precipitados e de deslocações para avaliação das hipóteses levantadas por meio de observações indiretas.

Além disso, propõe-se avaliar a seção longitudinal das amostras rompidas ou logo antes do rompimento em fadiga por flexão para observação das trincas. Desta forma, espera-se que seja possível observar as trincas ramificadas na fase R e trincas maiores na austenita.